



Deliverable No. 11.4

Validation of the CHIC infrastructure as a whole

Grant Agreement No.: 600841
 Deliverable No.: D11.4
 Deliverable Name: Validation of CHIC infrastructure as a whole
 Contractual Submission Date: 31/03/2017
 Actual Submission Date: 09/05/2017

Dissemination Level		
PU	Public	
PP	Restricted to other programme participants (including the Commission Services)	
RE	Restricted to a group specified by the consortium (including the Commission Services)	X
CO	Confidential, only for members of the consortium (including the Commission Services)	



COVER AND CONTROL PAGE OF DOCUMENT	
Project Acronym:	CHIC
Project Full Name:	Computational Horizons In Cancer (CHIC): Developing Meta- and Hyper-Multiscale Models and Repositories for <i>In Silico</i> Oncology
Deliverable No.:	D11.4
Document name:	Validation of the CHIC infrastructure as a whole
Nature (R, P, D, O) ¹	R
Dissemination Level (PU, PP, RE, CO) ²	RE
Version:	I (Final)
Actual Submission Date:	09/05/2017
Editor:	Georgios S. Stamatakis
Institution:	Institute of Communication and Computer Systems (ICCS) School of Electrical and Computer Engineering National Technical University of Athens (NTUA) <i>In Silico</i> Oncology and <i>In Silico</i> Medicine Group
E-Mail:	gestam@central.ntua.gr

ABSTRACT

This document reports on the validation of the CHIC infrastructure as a whole. Validation has been achieved mostly through the utilization and the execution of the three most computationally demanding clusters of highly innovative cancer *multimodeller*-hypermodels developed by the CHIC project. These three multiscale hypermodels address nephroblastoma, non small cell lung cancer and prostate cancer. The paradigmatic cancer types considered are treated with a variety of modalities including chemotherapy, radiation therapy and hormone therapy. In order to render the present document as concise as possible, without, however, losing generality, different aspects of the platform validation have been addressed by making use of possibly different hypermodels for different validation aspects. This is a justifiable approach since the present deliverable does not focus on the validation of each hypermodel *per se*, which has already been reported in detail in D6.4, but rather on the validation of the single CHIC infrastructure as a whole. This is achieved nevertheless, partly through particular examples of hypermodel validation. Therefore, the various testing and validation steps (addressing *inter alia* execution outcome reproducibility, consistency of the execution time demands of the same model with the same input on the same computational framework under the same computational load and error free hypermodel execution) are sometimes reported in the sections of different hypermodels. In specific exemplary cases, it is shown how the utilization of the infrastructure can support the conduction of the scientific validation of a hypermodel. The last chapter of the document outlines the technical components and the workflow used for the validation of the CHIC infrastructure as a whole. The overall outcome of the validation under consideration has been a successful one. Obviously, proper functioning of the infrastructure has been achieved through an intensive and lengthy error identification and fixing procedure, the latter being a standard approach in software engineering practice. It is noted that the evaluation of the CHIC infrastructure through the CHIC platform directly by the clinical community has already been conducted and reported in previous deliverables. Therefore this is not included in the present document.

¹ R=Report, P=Prototype, D=Demonstrator, O=Other

² PU=Public, PP=Restricted to other programme participants (including the Commission Services), RE=Restricted to a group specified by the consortium (including the Commission Services), CO=Confidential, only for members of the consortium (including the Commission Services)

KEYWORD LIST:

cancer modelling, multiscale cancer modelling, hypermodelling, CHIC project, hypermodel, hypomodel, component model, tumour growth, angiogenesis, cancer biomechanics, cancer metabolism, molecular cancer modelling, integrated cancer model, Oncosimulator, hypermodel based oncosimulator, *in silico* oncology, *in silico* medicine, systems medicine, computational oncology, computational medicine, systems oncology, finite element method, discrete event, discrete entity, partial differential equation, ordinary differential equation, semantics, model repository, clinical research application framework, CRAF, hypermodelling editor, hypermodel execution, nephroblastoma, non small cell lung cancer, glioblastoma multiforme, prostate cancer

The research leading to these results has received funding from the European Community's Seventh Framework Programme (FP7/2007-2013) under grant agreement n° 600841.

The author is solely responsible for its content, it does not represent the opinion of the European Community and the Community is not responsible for any use that might be made of data appearing therein.

MODIFICATION CONTROL

Version	Date	Status	Author
1.0	24/03/2017	Draft	G. Stamatakis, ICCS-NTUA
2.0	14/04/2017	Draft	G. Stamatakis, ICCS-NTUA
3.0	26/04/2017	Draft	G. Stamatakis, ICCS-NTUA
4.0	30/04/2017	Draft	G. Stamatakis, ICCS-NTUA
5.0	04/05/2017	Revision	G. Stamatakis, ICCS-NTUA
6.0	08/05/2017	Clinical Check	N. Graf, USAAR
7.0 → 1 (Final)	09/05/2017	Revision	G. Stamatakis, ICCS-NTUA

List of additional contributors

N.Tousert, ICCS	I. Karatzanis, FORTH	R. Niklaus, UBERN	C. Guiot, UNITO
E. Kolokotroni, ICCS	K.Nikiforaki, FORTH	N. Mcfarlane, BED	I. Stura, UNITO
E. Georgiadi, ICCS	V. Sakalis, FORTH	Xu Zhang, BED	R. Bohle, USAAR
K. Argyri, ICCS	E. Tzamali, FORTH	J. Grogan, UOXF	D. Shouka, USAAR
N. Christodoulou, ICCS	S. Bnà, CINECA	H. Byrne, UOXF	E. Ebert, USAAR
D. Dionysiou, ICCS	P. Buechler, UBERN	R.Radhakrishnan, UPENN	S. Gool, KUL
S. Sfakianakis, FORTH	D. Abler, UBERN	A. Ghosh, UPENN	

EXECUTIVE SUMMARY

The present deliverable reports on the validation of the CHIC infrastructure as a whole. Validation has been achieved through the utilization and the execution of the three *most* computationally demanding clusters of highly innovative cancer *multimodeller*-hypermodels developed by the CHIC project. These three multiscale hypermodels address nephroblastoma, non small cell lung cancer and prostate cancer. The paradigmatic cancer types considered are treated with a variety of modalities including chemotherapy, radiation therapy and hormone therapy. In order to render the document as concise as possible without, however, losing generality, different aspects of the platform validation have been addressed using possibly different hypermodels. This is a justifiable approach since the present deliverable does not focus on the validation of each hypermodel *per se* (already reported in detail in D6.4) but rather on the validation of the single CHIC infrastructure as a whole. Therefore, the various testing and validation actions (addressing *inter alia* execution outcome reproducibility, consistency of the execution time demands of the same model with the same input on the same computational framework under the same computational load circumstances and error free hypermodel execution) may have been reported in the sections of different hypermodels. In specific exemplary cases, it is also shown how the utilization of the infrastructure can support the conduction of the scientific validation of a hypermodel. In more detail, in the case of the nephroblastoma hypermodel, the reproducibility of model predictions when executed on the CHIC Clinically Relevant Application Framework (CRAF) along with the hypermodel execution time as a function of the simulated time are addressed. In the case of non small cell lung cancer, apart from addressing the previous two aspects, a qualitative assessment of the produced results and several facets of partial clinical validation of the hypermodel are presented. In the case of prostate cancer, computing time requirements and reproducibility issues are addressed in conjunction with the partial clinical validation of the particular hypermodel cluster. The last chapter of the document outlines the technical components and the workflow used for the validation of the CHIC infrastructure as a whole. In this context, the chapter briefly outlines CRAF, the model and tool repository, the *in silico* trial repository, the hypermodelling framework, the clinical data repository and the workflow used for the validation of the CHIC platform. The overall outcome of the validation under consideration has been a successful one. Obviously, proper functioning of the infrastructure has been achieved through an intensive and lengthy error identification and fixing procedure which is common in software engineering practice. It is noted that the evaluation of the CHIC infrastructure through the CHIC integrating platform directly by the clinical community has already been conducted and reported in previous deliverables. Therefore, it is not included in the present document.

Contents

Executive Summary	4
IN. INTRODUCTION	6
NB: THE NEPHROBLASTOMA HYPERMODEL AS USED FOR THE VALIDATION OF THE CHIC INFRASTRUCTURE AS A WHOLE	7
LC: THE NON SMALL CELL LUNG CANCER HYPERMODEL AS USED FOR THE VALIDATION OF THE CHIC INFRASTRUCTURE AS A WHOLE	10
PC: THE PROSTATE CANCER HYPERMODEL USED FOR THE VALIDATION OF THE CHIC INFRASTRUCTURE AS A WHOLE	20
TE: TECHNICAL COMPONENTS AND THE WORKFLOW USED FOR THE VALIDATION OF THE CHIC INFRASTRUCTURE AS A WHOLE	31
DI: DISCUSSION	46
CO: CONCLUSIONS	47
APPENDIX I (ABBREVIATIONS AND ACRONYMS)	48

CHAPTER IN: INTRODUCTION

(Please note that the numbering of sections, subsections, equations, figures and references within this chapter refers exclusively to the latter and is not applicable to other chapters of the document, If any of the above entities of another chapter is to be referred to, the chapter under consideration should also be mentioned through its two capital letter code)

An important task of the CHIC project has been the validation of the various approaches, strategies, algorithms, mathematical and computational models, components and technologically integrating platforms. The present deliverable reports on the validation of the CHIC infrastructure as a whole. Validation in this sense has been largely achieved through the utilization and the execution of the three most computationally demanding clusters of highly innovative cancer *multimodeller*-hypermodels that have been developed by the CHIC project. These multiscale hypermodels address nephroblastoma (Chapter NB), non small cell lung cancer (Chapter LC) and prostate cancer (Chapter PC). These paradigmatic cancer types considered in this document are treated with a variety of modalities including chemotherapy, radiation therapy and hormone therapy.

In order to render the document as concise as possible, without, however, losing generality, different aspects of the platform validation have been addressed using generally different hypermodels. This is a plausible approach since the present deliverable does not focus on the validation of each hypermodel *per se* (already reported in detail in D6.4) but rather on the validation of the single CHIC infrastructure as a whole. Therefore, the various testing and validation actions (addressing *inter alia* execution outcome reproducibility, consistency of the execution time demands of the same model with the same input on the same computational framework under the same computational load circumstances and error free hypermodel execution) are possibly reported in the sections of different hypermodels. In specific exemplary cases, it is also shown how the utilization of the infrastructure can support the conduction of the scientific validation of a hypermodel.

In more detail, in the case of the nephroblastoma hypermodel, the reproducibility of model predictions when executed on the CHIC Clinical Relevant Application Framework (CRAF) along with the hypermodel execution time as a function of the simulated time are addressed. In the case of the non small cell lung cancer, apart from addressing the previous two aspects, a qualitative assessment of the produced results and several facets of partial clinical validation of the hypermodel are presented. In the case of prostate cancer, computing time requirements and reproducibility issues are addressed in conjunction with the partial clinical validation of the particular hypermodel cluster.

The last chapter of the document (Chapter TE) outlines the technical components and the workflow used for the validation of the CHIC infrastructure as a whole. In this context, the chapter briefly outlines CRAF, the model and tool repository, the *in silico* trial repository, the hypermodelling framework, the clinical data repository and the workflow used for the validation of the CHIC platform.

The overall outcome of the validation under consideration has been a successful one. Consistent and stable functioning of the infrastructure has been achieved through an intensive and lengthy error identification and fixing procedure, being commonplace in software engineering.

It is also be noted that the evaluation of the CHIC infrastructure and platform directly by the clinical community has already been reported in previous deliverables and therefore it is not included in the present report.

CHAPTER NB: THE NEPHROBLASTOMA HYPERMODEL AS USED FOR THE VALIDATION OF THE CHIC INFRASTRUCTURE AS A WHOLE

(Please note that the numbering of sections, subsections, equations, figures and references within this chapter refers exclusively to the latter and is not applicable to other chapters of the document, If any of the above entities of another chapter is to be referred to, the chapter under consideration should also be mentioned through its two capital letter code)

I. Validation of the Nephroblastoma multimodeller hypermodel execution through the CHIC infrastructure

I.1 Reproducibility

Four executions for the same patient with the same hypermodel configurations have been submitted to the infrastructure through CRAF in order to check the reproducibility of the system. The execution of the model was successful at all times.

The mean execution time for modeling a patient with initial image (array) size after processing of 52*59*74 (227032 voxels) for a simulation period of 29 days has been estimated to 7.5 min.

Table I. Reproducibility results

Simulation #	Predicted Volume reduction (%) of initial tumour)	Execution time (min)
1	81.06	7
2	81.18	8
3	81.04	7
4	81.15	8

The standard deviation of the predictions on the tumour volume reduction is 0.06%.

The time evolution of the tumour volume as simulated at those 4 executions is figured in Fig I and is the similar for all executions.

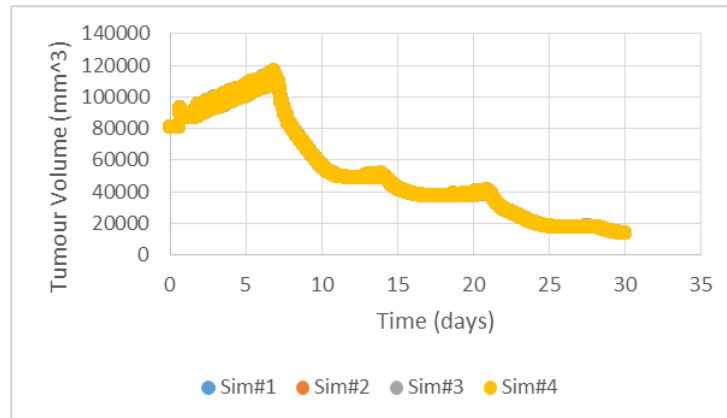


Fig I Tumour volume time evolution simulated from several model executions with the same running configurations.

Concluding, the study verifies that the hypermodel is characterized by a high reproducibility in the sense that repeated executions under unchanged conditions yield the same results.

1.2 Execution time demands

A short study on the execution time demands of the Nephroblastoma Multimodeller Hypermodel has been made. The execution time strongly depends on the size of the personalized image of the patient used as input and the simulation period. The communication frequency between the hypomodels has been considered constant. All executions of Wilms Multimodeller Hypermodel have been submitted through CRAF.

Five simulations have been submitted with different simulation periods and the execution time has been estimated for the same input image size. The results are presented in fig 2.

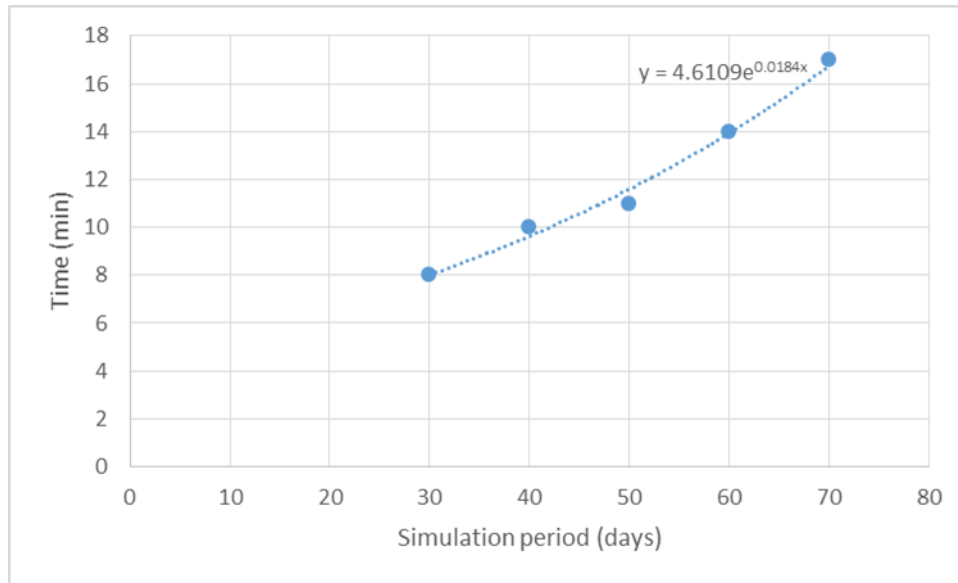


Fig 2. Execution time as a function of Nephroblastoma Hypermodel simulated time.

CHAPTER LC: THE NON SMALL CELL LUNG CANCER HYPERMODEL AS USED FOR THE VALIDATION OF THE CHIC INFRASTRUCTURE AS A WHOLE

(Please note that the numbering of sections, subsections, equations, figures and references within this chapter refers exclusively to the latter and is not applicable to other chapters of the document, If any of the above entities of another chapter is to be referred to, the chapter under consideration should also be mentioned through its two capital letter code)

I. Non Small Cell Lung Cancer Hypermodel Validation

I.1 Lung Cancer Multimodeller Hypermodel

I.1.1 Reproducibility

The Lung Hypermodel was launched four times for the same patient and with the same values of input arguments through CRAF. The hypermodel was configured and launched successfully all of the times. Based on the results, the four simulated time courses of tumour volume are the same (Fig.1). Furthermore, the tumours of the four simulations at an indicative simulation day (day 98 has been chosen here for demonstration purposes) have the same shape (Fig 2). The predicted volume reduction is reported in Table I. The deviation between the predictions is below 0.003%. Finally, the execution time is approximately one hour in all cases. Concluding, the study verifies that the hypermodel is characterized by a high precision in the sense that repeated executions under unchanged conditions yield the same results.

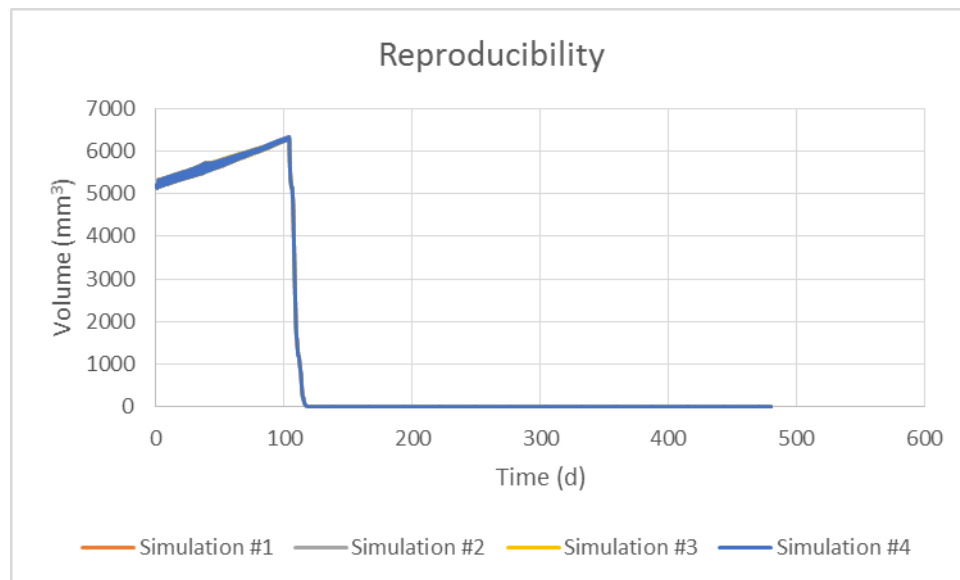


Fig I. Simulated time course of tumour volume

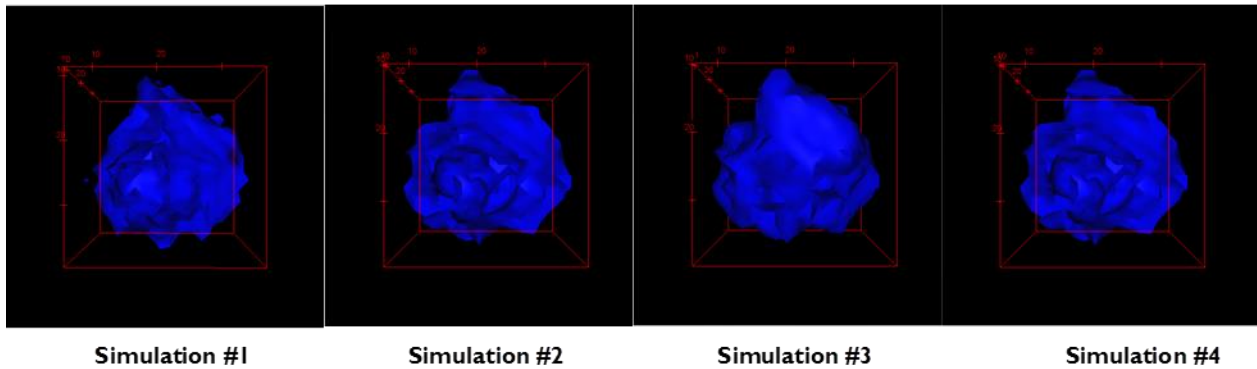


Fig 2. 3D presentation of the simulated tumour at day 98 (date of second imaging time point, before irradiation).

Table I. Reproducibility results

	Predicted Volume reduction (% of initial tumour)	Execution time (min)
Simulation #1	99.9789	62
Simulation #2	99.9795	61
Simulation #3	99.9795	56
Simulation #4	99.9815	56

1.1.2 Execution Time Demands

The execution time depends on the size of the reconstructed tumour image and the simulation period. The mean execution time for an initial image of size after processing of $44 \times 45 \times 48$ (92928 voxels) and for a simulation period of 480 days is approximately one hour. The execution time as a function of simulation time is depicted in Fig 3.

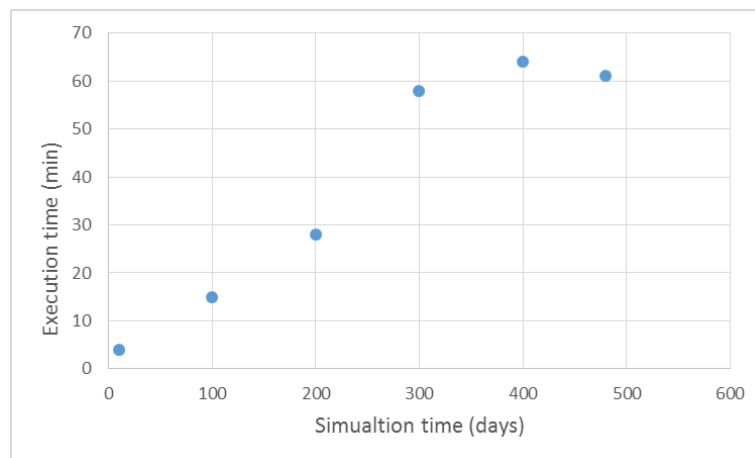


Fig 3. Execution time as a function of Lung Hypermodel simulation time.

I.1.3 Qualitative Assessment of Results

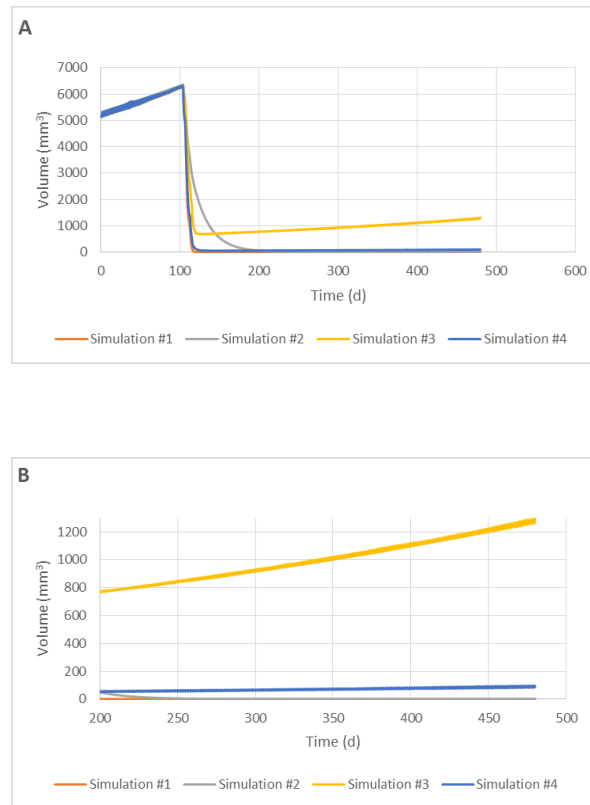
The lung patient considered has been simulated for four indicative value combinations of input scalar arguments. The aim is to assess the potential of the hypermodel to produce qualitatively reasonable results. More specifically, the clinical case was simulated assuming different values of loss rate of terminally differentiated cells, radiation dose and oxygen enhancement ratio. In Fig 4 simulation #1 is the reference value combination of input arguments, whereas simulations # 2, 3, 4 correspond to a lower loss rate of terminally differentiated cells, a lower radiation dose and a higher oxygen enhancement ratio, respectively.

A long life expectancy of terminally differentiated cells (reflected in a low loss rate) is associated with a high portion of differentiated cells to stem and progenitor cells. Furthermore, because radiation targets cells with proliferative capacity, treatment-induced reduction in differentiated cell population appears with a delay. As a result, a sufficiently low loss rate of differentiated cells results in a more gradual decrease in tumour volume (Fig 4A: simulation #2 compared to simulation #1).

The hypermodel successfully demonstrated a worse treatment response and a faster tumour cell repopulation with decreasing radiation dose (Fig 4A: simulation #3 compared to simulation #1).

Cell radiosensitivity varies considerably throughout the cell cycle. In our modelling approach, oxygen enhancement ratio (OER) is the parameter that regulates the radioresistance of dormant (G0) and synthesis (S) phase compared to the rest of the proliferative phases (G1, G2, M). Higher OER results in less G0 and S-phase cells lethally hit by radio and, hence, a tumour of bigger size at the end of the simulation (Fig 4B: simulation #4 compared to simulation #1).

Concluding, qualitatively an expected and reasonable behaviour of virtual tumour response to radiation treatment has been demonstrated in all experiments.



VALUES OF SCALAR INPUT ARGUMENTS RELATED TO FREE GROWTH AND CYTOTOXICITY. IN BOLD THE ARGUMENTS THAT WHERE VARIED BETWEEN EXECUTIONS

Parameter	#1	#2	#3	#4
Nutrient consumption rate	7.6e-9 h ⁻¹	7.6e-9 h ⁻¹	7.6e-9 h ⁻¹	7.6e-9 h ⁻¹
Nutrient diffusivity	0.396 mm ² /h	0.396 mm ² /h	0.396 mm ² /h	0.396 mm ² /h
Nutrient concentration in non tumour regions.	0.9	0.9	0.9	0.9
Cell cycle duration	40 h	40 h	40 h	40 h
Duration of dormant phase	168 h	168 h	168 h	168 h
Time needed for necrosis products to disappear	23 h	23 h	23 h	23 h
Time needed for apoptosis products to be removed	4 h	4 h	4 h	4 h
Number of mitoses performed by LIMP cells before differentiation	22	22	22	22
Apoptosis rate of stem and LIMP cells	0.001 h ⁻¹	0.001 h ⁻¹	0.001 h ⁻¹	0.001 h ⁻¹
Apoptosis rate of differentiated cells	0.017 h⁻¹	0.001 h⁻¹	0.017 h⁻¹	0.017 h⁻¹
Necrosis rate of differentiated cells	0.025 h⁻¹	0.001 h⁻¹	0.025 h⁻¹	0.025 h⁻¹
Fraction of G0 cells that re-enter cell cycle	0.1	0.1	0.1	0.1
Fraction of cells that enter G0 phase following mitosis	0.263	0.263	0.263	0.263
Fraction of stem cells that perform symmetric division	0.322	0.322	0.322	0.322
Radiation Dose	15 Gy	15 Gy	5 Gy	15 Gy
Oxygen enhancement ratio	1	1	1	3

Fig 4. Hypermodel results for four indicative value combinations of input scalar arguments. A. Time course of tumour volume during the whole simulation period. B. Time course of tumour volume during the last 280 days.

I.1.4 Partial Clinical validation

I.1.4.1 Clinical Scenario: Neoadjuvant Chemotherapy for Resectable Non-Small-Cell Lung Cancer

The Lung Oncosimulator has been adapted and partially validated based on 12 NCSLC (adenocarcinoma and squamous cell carcinoma) cases treated preoperatively with a cisplatin-based doublet regimen (for more details see D6.4). The patient specific data that have been exploited to clinically adapt the Lung Oncosimulator are the applied chemotherapeutic schemes (drugs, administration instants) and the 3D images of the clinical tumours as segmented and reconstructed from the available CT imaging data. The sets of imaging data refer to the primary tumours and were provided for two time instances before, and during or after the completion of the systemic treatment (prior to surgery). During adaptation, two cohorts of virtual tumours have been defined corresponding to two typical proliferation profiles, one for adenocarcinoma and one for squamous cell carcinoma histological types. The two typical proliferation profiles have been defined based on literature. For each patient and virtual tumour of the corresponding profile, the regimen's cytotoxicity has been adapted to achieve the observed treatment-induced reduction in tumour volume.

Following adaptation, an early validation has been attempted, by comparing the post-surgical excision measurements with the simulated tumour size at the time of surgery (Fig 5). In particular, for each clinical case and for each virtual tumour/regimen's cytotoxicity pair, an extended simulation has been performed starting from the first CT acquisition until the date of surgery. A good agreement between the prediction and the actual data is observed for the six out of twelve cases (for more details see D6.4).

By taking into account the existence of uncertainties in estimating the true tumour volume, the limited number of data sets available for the estimation of cytotoxicity and the consideration of a single proliferation profile differentiated only on the grounds of the two histological subtypes of the available clinical cases, the gross agreement between the predicted tumour values and the post-surgery measured ones indicate that the proposed model has a clear clinical potential.

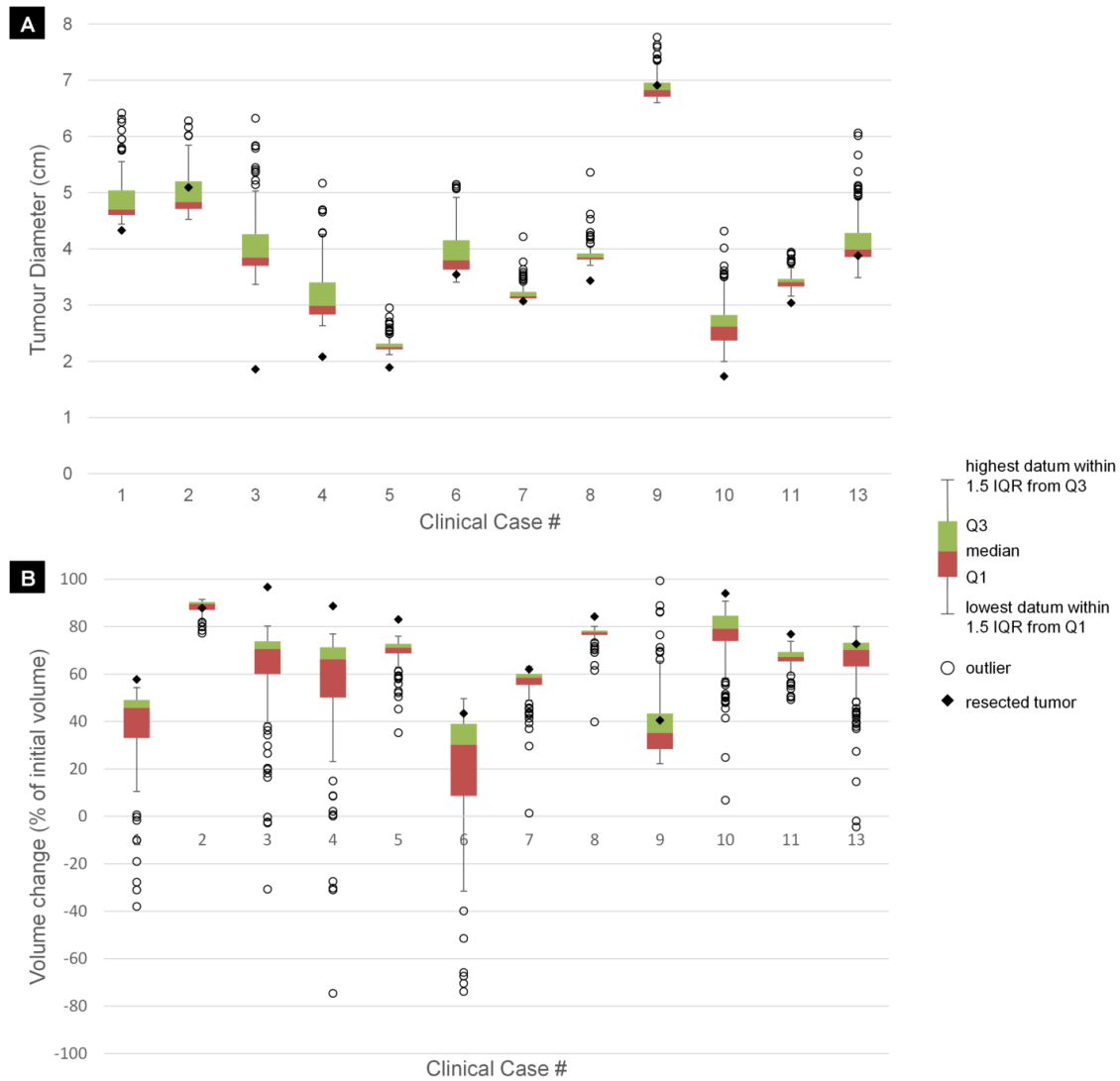


Fig 5. Box-and-whisker plots of model predictions at the time of surgery for the clinical cases. Each box and whisker plot corresponds to N (146 and 175 for the SCC and ADC cases respectively) independent predictions. Each prediction results from an extended model simulation starting from the first CT examination till the time of surgery. The simulations have assumed the virtual tumours and corresponding cytotoxicities derived during the adaptation phase. At any given case the horizontal line between the green and the red boxes denotes the median (50th percentile) of the N predictions, the lower boundary of the red box and the upper boundary of the green box denote the first (Q1) and third (Q3) quartiles, whereas the predictions more than 1.5 interquartile (IQR) distance from the end of the boxes are denoted as outliers (depicted as circles). The whiskers extend from the lowest to the highest prediction that falls within 1.5 IQR from the outer edge of the boxes. The predictions correspond to (A) the equivalent diameter of the tumour at the time of surgery, defined as the diameter of a sphere with the same tumour volume as the predicted one and (B) the absolute value of the volume change of the tumour, expressed as a percentage of the initial volume. For the clinical case # 9 the volume change corresponds to an increase, whereas for rest cases to a reduction. The corresponding values derived by the measurements of the surgical resected tumour are denoted as a filled rhomb.

I.1.4.2 Case scenario: Progression and response to treatment of recurrent Non-Small-Cell Lung Cancer

The Lung Multimodeller Hypermodel has been adapted and partially validated with a recurrent NCSLC adenocarcinoma case treated with irradiation (for more details see D6.4). The clinical question addressed by the Hypermodel concerns the prediction of volume reduction of the tumour one year following the completion of tumour irradiation. The patient specific data that have been exploited are his/her mutation data, miRNA data, proliferation index, the applied radiotherapeutic scheme (dose, radiation instants) and the imaging studies of the recurrent tumour before irradiation. A cohort of virtual tumours with common, patient-specific proliferation characteristics, i.e. growth fraction and volume doubling time, has been defined. The 3D image of the tumour and surrounding healthy tissue has been reconstructed from the dicom series. The hypermodel has been executed for each virtual tumour and the tumour size one year following irradiation has been evaluated (Fig 6). The hypermodel predicts a tumour of approximately 1mm i.e. a tumour not easily identified. Based on patient data no visible tumour exists one year after irradiation. Even-though hypermodel predictions seem consistent with reality, follow-up data beyond this period would be needed to properly validate the hypermodel, for the specific clinical case.

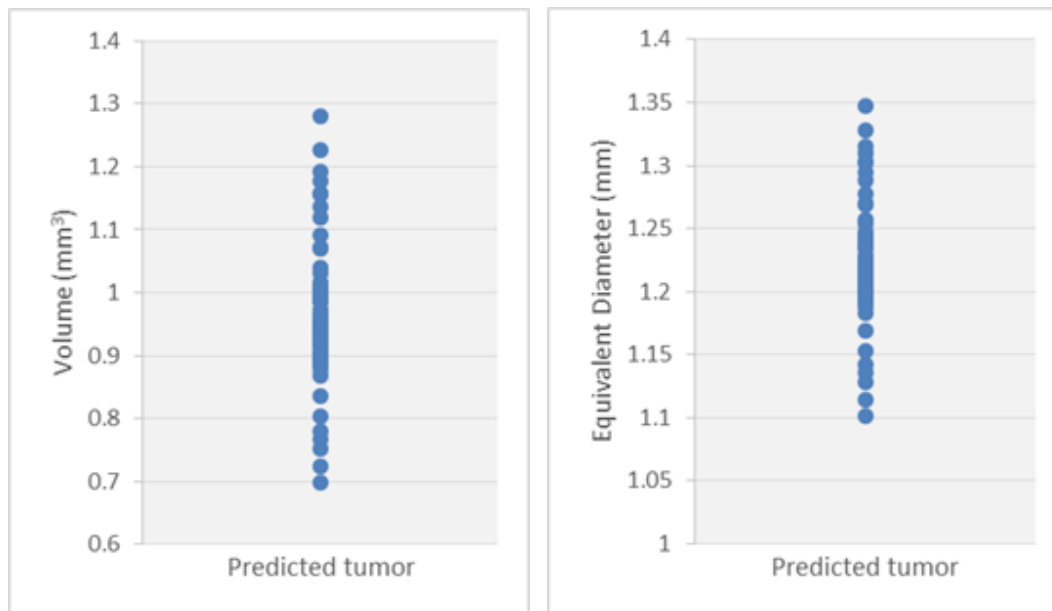


Fig 6. Predicted tumour size one year after irradiation

The 3D presentation of the simulated tumour for an indicative execution has been compared to the 3D reconstructed image of the real tumour at the date of second imaging time point (simulation day 98 - before irradiation) (Fig 7). The simulated growing tumour maintains a compact shape, in agreement with observation. Its simulated and observed position at the second imaging time point are approximately 2 cm apart. Concluding, the hypermodel is found to reproduce realistic tumour shapes in the specific growth scenario; however, reliable prediction of tumour shape and position with the developed approach and the available information is not yet possible.

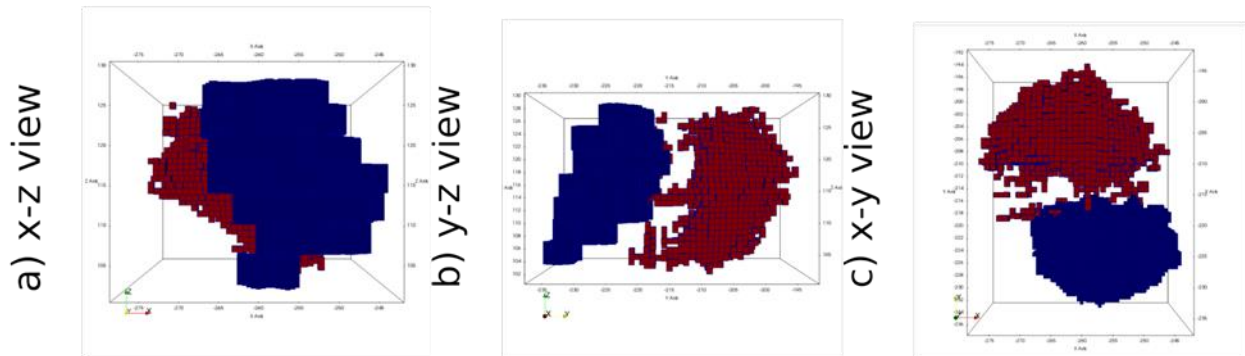


Fig 7. Visual comparison of shape and position between simulated (red) and observed (blue) tumour at the respective second imaging time point. During the simulation period, the tumour volume increases.

1.2 Lung Cancer Statistical Approach

In the context of CHIC, two classifiers have been developed aiming to predict whether a surgically treated NSCLC patient will relapse. More specifically the clinical question posed is: Will a Lung Cancer patient with NSCLC adenocarcinoma suffer from tumour recurrence after surgical resection?

1.2.1 Execution Time Demands

The models take a few seconds to run on CHIC platform.

1.2.2 Classifier #1

A Naïve Bayes classifier has been trained based on the expression data of 10 miRNAs and particularly the fold-change of the normalized expression values between tumour and normal tissue. The accuracy of the classifier has been validated based on the leave-one-out cross-validation method on a set of 10 patients with known recurrence. Its accuracy reaches 100% (Table 2). Even though the results are promising, no definite conclusions can be drawn, due to the small size of the sample.

Table 2. Confusion matrix of Naïve Bayes performance

		Predicted class		
		complete remission	recurrence	Recognition
Actual class	complete remission	4	0	100%
	recurrence	0	6	100%
	Precision	100%	100%	

1.2.3 Classifier #2

A Neural Network classifier has been trained based on age, stage and the expression data (the fold-change of the normalized expression values between tumour and normal tissue) of 6 miRNAs which are over or under expressed in tumour compared with normal tissue. The classifier has been trained and validated on a training set of 14 patients. The accuracy of the classifier estimated based on the leave-one-out cross-validation method is 71.43% (Table 3). Furthermore, it predicts with an accuracy of 80% the recurrence in a separate test set of 5 patients with visible tumour at some point after surgery (Table 4). Even though the results are promising, no definite conclusions can be drawn, due to the small size of the training and test set.

Table 3. Confusion matrix of Neural Network performance on the training set

		Predicted class		
		complete remission	recurrence	Recognition
Actual class	complete remission	5	3	62.50%
	recurrence	1	5	83.33%
	Precision	83.33%	62.50%	

Table 4. Neural Network performance on the test set

Patient #	Prediction	Confidence (no)	Confidence (yes)	Actual class
1	no	0.7834	0.2163	yes
2	yes	0.00564	0.99436	yes
3	yes	0.3807	0.6193	yes
4	yes	0.0951	0.9049	yes
5	yes	0.0003	0.9997	yes

CHAPTER PC

THE PROSTATE CANCER HYPERMODEL USED FOR THE VALIDATION OF THE CHIC INFRASTRUCTURE AS A WHOLE

(Please note that the numbering of sections, subsections, equations, figures and references within this chapter refers exclusively to the latter and is not applicable to other chapters of the document, If any of the above entities of another chapter is to be referred to, the chapter under consideration should also be mentioned through its two capital letter code)

I. Prostate Multimodeller Hypermodel Validation

Radical prostatectomy (RP) is one of the most widespread curative treatments for localized Prostate Cancer (PCa), but tumour recurrence affect almost 20% of patients.

In case of high-risk patients, with either advanced pathological stage, or positive surgical margins or regional lymph node metastasis or Gleason score ≥ 8 recurrence may occur quite early after RP, and adjuvant treatments (i.e. immediately subsequent RP) are delivered, mainly consisting in hormonal therapy.

The underlying rationale is based on the fact that, as recognized by Huggins and Hodges more than 70 years ago, PCa is an androgen-sensitive disease, and different approaches to reducing testosterone (bilateral orchiectomy, chronic administration of gonadotropin releasing hormone analogs, etc.) collectively indicated as androgen deprivation therapy (ADT), are nowadays considered as standard therapy at recurrence.

For adjuvant ADT in RP patients neither conclusive support for benefits nor standard recommendations (www.nccn.org) exist.

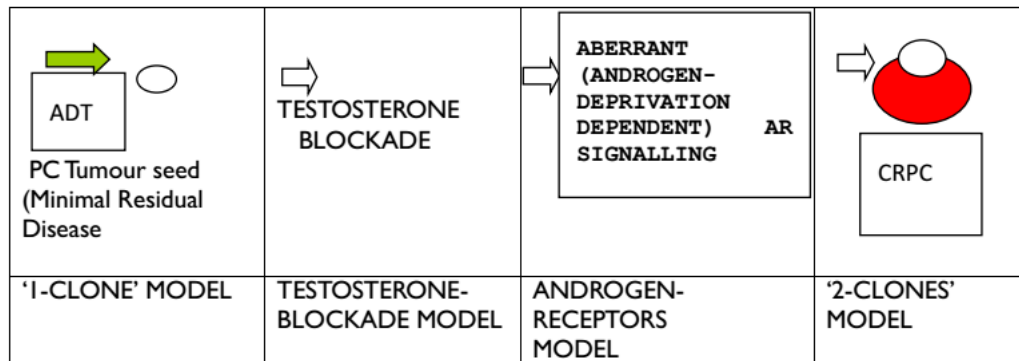


Figure 1: Schema of the 2-clones model construction

The novelty of the present joint work is the implementation of the mathematical simulation of the different action of LHRH agonists (shortly: LHRH). Another essential point is that theoretical results are compared with clinical data available by EUREKA1 study.

1.1 Simulation of testosterone blockade by LHRH agonists

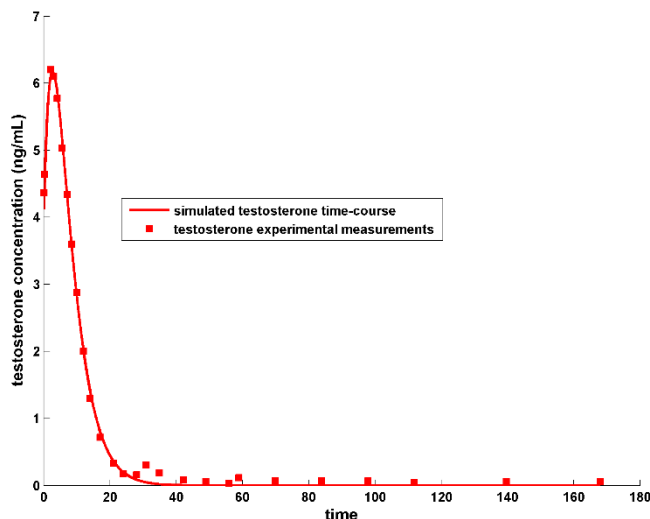


Fig. 2 Fitting of the pharmacodynamic hypo-model to testosterone concentration data in (Marberer et al. 2010). Parameter values and initial values are shown in Tables 4 and 3 respectively. The normalized root mean square error, defined as the root mean square error divided by the range of values of the measured quantity (maximum value – minimum value), was calculated equal to 5.24%.

1.2 The Androgen Receptors and the genesis of castration-resistant cancer cells AND patient-specific predictions of cell growth and death probabilities (rates) using the patient genomic profiles and the molecular model

Gene expression data for 20 patients were utilized using which the nodes of the molecular model were initialized individually for each subject. In Table I, the genes that were differentially expressed compared to a control (healthy subject) are given for 4 out of the 20 patients. The remaining 16 patients did not show any differentially expressed genes relative to the control subject. For each patient, the gene names on the right column were obtained from gene expression data by comparing the gene expression with normal (healthy subject with no cancer) and picking the top 20 differentially expressed genes. These gene activities/concentrations were altered in our simulation.

Patient ID	Differentially Expressed Genes WRT Control	DGEP (Y/N)?
CNT or Control	NA	N
AA65	CCNG1;CDKN1A;MDM4;CDK2	Y
Z59	CCNG1;CDKN1A;CDK2;CASP9	Y
AA69	CCNG1;CDKN1A;CDK2	Y
L12	CCNG1;CDKN1A;AR;CASP9	Y
B17	CCNG1;CDK2;AR;MDM4	Y
A3	CCNG1;CDK2;AR;MDM4	Y
W25	CCNG1;CDKN1A;CDK2;CASP9	Y
A5	CCNG1;CDKN1A;CDK2;CASP9	Y
B11	CCNG1;CDKN1A;MDM4;CDK2	Y
G70	None	N
C25	None	N
CC87	None	N
CC8	None	N

Table I. Patient gene expression profiles showing top differentially expressed genes compared to a control (healthy) subject without cancer. The colours represent patients with similar patterns of differentially expressed genes. So patients shown is same colour can in principle be stratified into a cohort. For the purposes of this study, we pool all patients with differentially expressed genes into one cohort. These are indicated DGEP=Y in the last column. Thus, two patient cohorts we consider here are represented by DGEP=Y and DGEP=N.

1.3 The two cancer cell populations growth model

The starting hypothesis is that the tumour is in an initial phase (tumour seed or Minimal Residual Disease after surgery), i.e. it grows with an exponential law $dC_t(t)/dt = r_t \cdot C_t(t)$.

In case of a delayed treatment, the growth can be modelled with the Gompertzian or West's law.

Following prostatectomy, if tumour seeds are still present, the 'testosterone-sensitive' population S grows with testosterone-dependent growth rate r:

$$r = r_0 + p T \quad (1)$$

In the absence of any therapy, a standard (and constant) T_0 value is assumed.

In case of ADT, we should consider two different scenarios. When a LHRH –agonist treatment is performed the Equation becomes:

$$1/S \, dS/dt = r(t) = r_0 + p T(t) \quad (2)$$

$T(t)$ being the testosterone concentration in plasma, given by the result of the TESTOSTERONE-BLOCKADE' model. This function, also addresses the 'testosterone flare' observed in the first week following LHRH therapy.

The effect of the AR-blocking anti-androgen therapy on both the PSA and testosterone production can be modelled in similar, but not identical, way.

In the case of LHRH and combined therapy a resistant clone of tumour cells is expected to develop. Its contribution, more than increasing the PSA production, is expected to enhance tumour progression. Its mathematical expression is given by

$$dR/dt = (r_0 + a(K - S)/K) R \quad (3)$$

a being the additional tumour rate and K its carrying capacity.

The prostate cancer growth follows a Gompertzian law characterized by an initial exponential growth prior to its reaching a carrying capacity. We need to consider this type of behaviour if we are studying the entire period of life of the tumour. In this work, however, we consider only the first part of re-growth, so when the initial population is very small and the growth is exponential. The carrying capacity depends on the nutrients of the body and the available space. It still exists, but it is huge comparing to tumour size, so we can ignore it. If two populations are growing in the same site, however, we need to take into account that the two clones compete for the same nutrients and the same space. We can do it considering the carrying capacity.

The 'additional' rate, as well as carrying capacity, are due to the Castration Resistant cells.

The total PSA value is evaluated as:

$$PSA(t) = S_{coeff} * S(t) + R_{coeff} * R(t) \quad (4)$$

The parameter values are reported in Table 2 .

Table 2: Parameter values definition and numerical simulations

Parameter	Values from the literature
r_0	$0.155 \pm 0.12 \text{ month}^{-1}$ (from UPENN model)
p	$0.01 \pm 0.008 \text{ cell}^{-1}$ (from UPENN model)
a	0.35 ± 0.02 (from UPENN model)
T_0	Between 0.09 and 0.21 g/month in (Vierhapper et al. 1997)
$T(t)$	Function from the 'TESTOSTERONE-BLOCKADE' model
K	Local/metastatic values, in our simulations = 200 ng/mL
Scoeff	$0.145 \cdot 30 \text{ ag/mL/cell/month}$ (production rate of R: 0-0.29 ag/mL/cell/day in (Morken et al. 2014))
Rcoeff	$0.1825 \cdot 30 \text{ ag/mL/cell/month}$ (production rate of R: 0.015-0.35 ag/mL/cell/day in (Morken et al. 2014))

In the LHRH and combined models, the resistant population R always increases unless $R_0=0$.

Based on the results of Figures 8 and 9, we can summarize the following

- For S cells, the testosterone independent growth probability is 0.016 for control subject; we assume this maps to the $r_0=0.028 \text{ month}^{-1}$ for control subjects given in Table 2.
- For S cells, the mean value the testosterone independent growth probability for DGEP subjects is 0.155; hence, r_0 for DGEP subjects = 0.271 month^{-1} ($=0.155 \cdot 0.028 / 0.016$)
- For S cells, the testosterone-dependent growth probability calculated as delta NCG high T minus low T for control subject = 0.505; this allows us to estimate p as follows. The testosterone-dependent rate is pT which corresponds to the testosterone-dependent growth probability of 0.505; this equivalence yields $pT/r_0=0.505/0.016$ or $pT=(0.505/0.016) \cdot 0.028 \text{ month}^{-1}$. The testosterone concentration for this calculation was 20 nM (or 8 ng/ml) which yields the value for $p=(0.505/0.016) \cdot (0.028/8)=0.11 \text{ month}^{-1} \text{ ng}^{-1} \text{ ml}$.
- For S cells, the mean testosterone-dependent growth probability calculated as mean delta NCG high T minus low T over all DGEP subjects = 0.444; this results in $p=(0.444/0.155) \cdot (0.271/8)=0.09 \text{ month}^{-1} \text{ ng}^{-1} \text{ ml}$ for DGEP subjects.
- For R cells under no competition, the growth rate is r_0+a which we take to be proportional to the mean NCG for high and low T under low PTEN (here, low

PTEN is taken to be the marker of resistance). Based on this equivalence, we can estimate a for control and DGEP subjects, see below.

- For R cells, the mean value for NCG for control subject=0.402 (obtained from averaging NCG for low and high T for control). Therefore, for control subjects $(r_0+a)/(r_0)=\text{mean NCG for R cells}/\text{NCG for S cells under low T}$; hence, $1+(a/r_0)=0.402/0.016$, which yields $a=24.125*r_0=24.125*0.028 \text{ month}^{-1}=0.6755 \text{ month}^{-1}$.
- For R cells, the mean value for NCG for DGEP subjects=0.5055 (obtained from averaging NCG for low and high T for each DGEP subject and then taking the mean over the DGEP subjects). Therefore, for DGEP subjects $(r_0+a)/(r_0)=\text{mean NCG for R cells}/\text{NCG for S cells under low T}$; hence, $1+(a/r_0)=0.5055/0.155$, which yields $a=2.26*r_0=2.26*0.271 \text{ month}^{-1}=0.613 \text{ month}^{-1}$.

1.4 Model validation Vs EUREKAI database: PSA values prediction

The EUREKAI data collection contains a subset of prostatectomized patients who were considered as high-risk ones, based on their Gleason Score values ($GS \geq 8$) and the positive surgical margins. Those for which at least 4 PSA postoperative values were available, and info about the biochemical relapse were reported were selected for the present study.

Some of them underwent ADT adjuvant therapy either with LHRH or with AR-blocking drugs, in contrast to a control group of patients without any adjuvant therapy.

In order to check whether the parameter values cited in the literature agree with those validated on the EUREKAI patients we selected some particular subsets for whom the evaluation of the above parameters was much sensible.

i) Validation of r_0

The timing of testosterone concentration depends on the phase of the LHRH therapy, and in particular T can be assumed to be negligible after the initial flare.

Consequently, we selected 60 patients undergoing LHRH therapy for whom at least two values of the PSA dosage were available during the therapy.

Assuming that $T(t) = 0$ $r = r_0$ can be easily evaluated assuming an exponential tumour growth, independently of the value of Scoeff.

We found r_0 in the same range as expected from the literature and from UPENN model.

ii) Validation of pT without therapy

Assuming that no ADT was administered, we expect that both the testosterone production and its consumption for tumour growth are physiologically distributed on the population.

In order to estimate it on the EUREKA1 database, we selected 84 relapsed patients who didn't undergo any therapy and had at least 2 PSA values after RP.

Assuming $r_0 = 0.02 \text{ month}^{-1}$ we found $pT = (0.04 \pm 0.07) \text{ month}^{-1}$, which is compatible with the assumption of $p = 0.01 \pm 0.008 \text{ cell}^{-1}$ and a low value of testosterone (3.7 mg/day). Figs 3a and 3b describe the 'true' and 'theoretical' curves respectively.

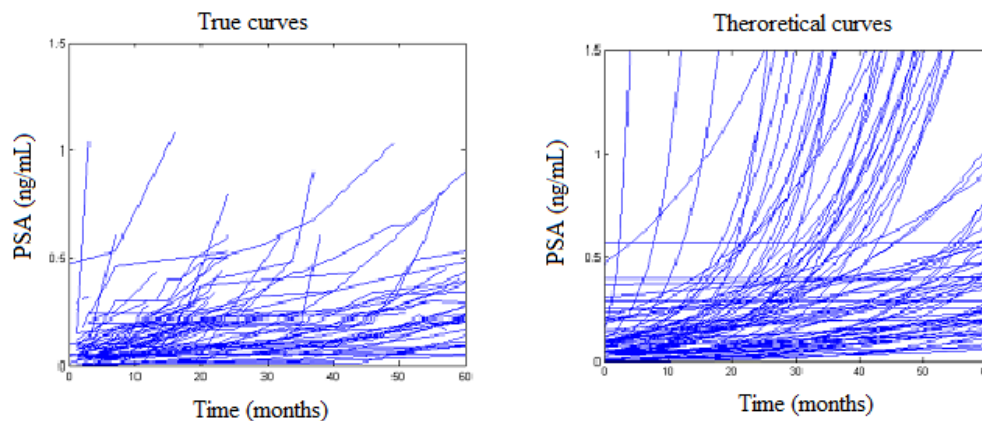


Figure 3a true curves; 3b theoretical curves.

1.5 Output description

The hypermodel gives 5 different previsions for each scenario, changing the parameter values according to their ranges. This happens because we want to give an idea of the behaviour of the PSA, but we cannot expect to predict the exact future PSA values. If extra information is available, for example gene expression, the prediction can be more accurate and the most probable scenario can be easily selected.

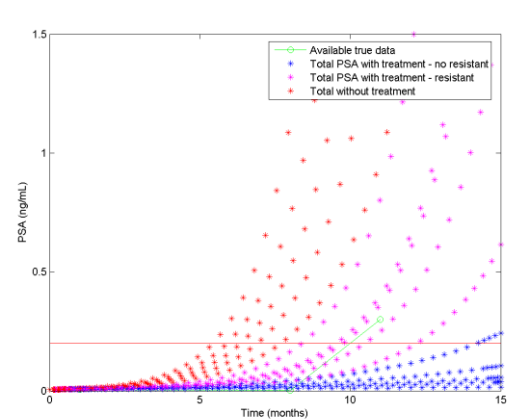
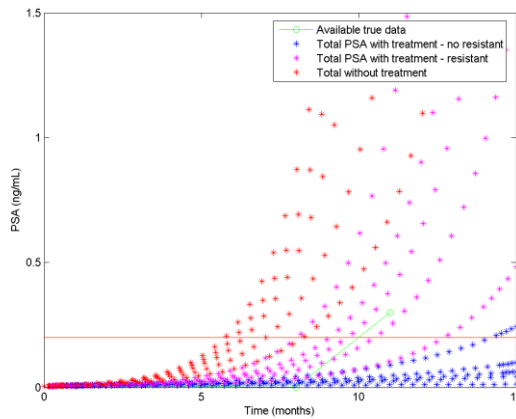
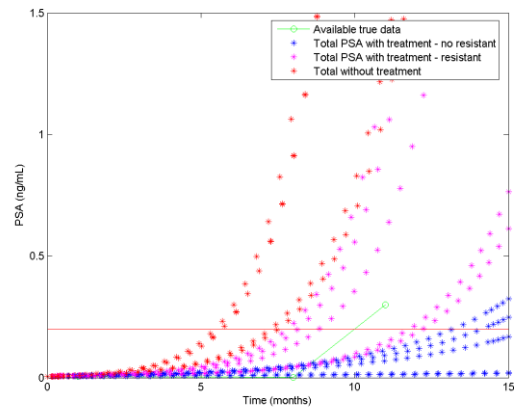
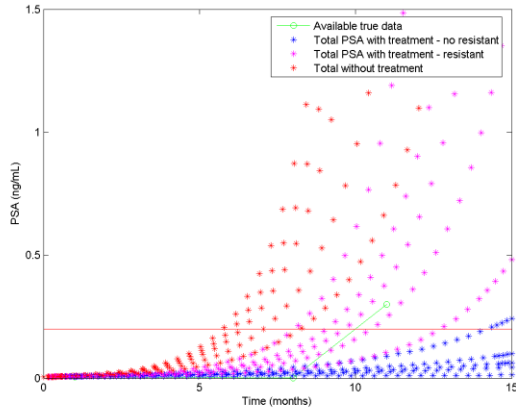
To be precise, the output of the hypermodel is a .png file with 5 execution of the 3 scenarios:

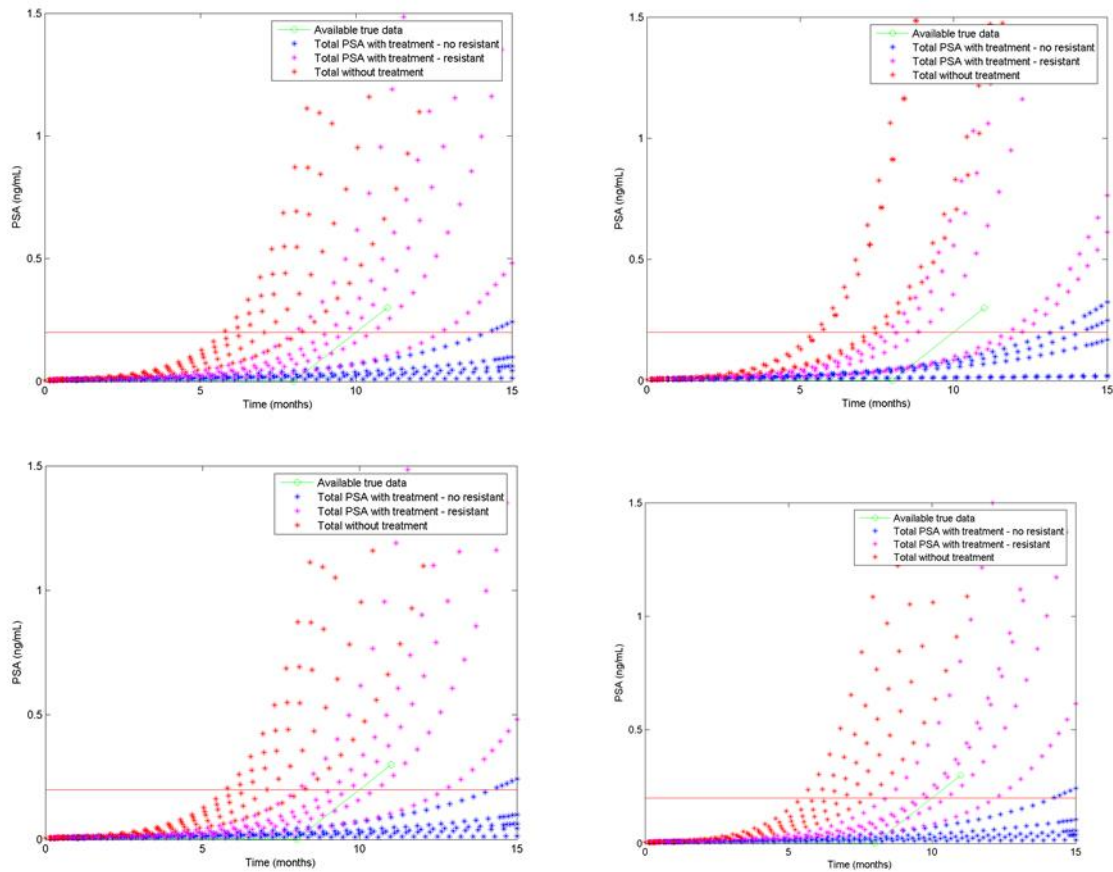
1. Blue stars: successful treatment, in which the resistant population is very small or it is not present
2. Magenta stars: unsuccessful treatment, in which the resistant population is large and recurrence can be observed during the treatment
3. Red stars: no treatment, with no resistant population

In this way, the clinician can see the different scenarios in comparison with the available real data (in green).

1.6 Reproducibility

The Prostate Hypermodel was launched four times for the same patient and with the same values of input arguments through CRAF. The hypermodel was configured and launched successfully all of the times. Each time the patient was classified correctly as a 'bad responsive' (magenta stars).





I.7 Execution time demands

The execution time does not depend on the data. Moreover less than 5 minutes are necessary for each run.

I.8 Partial clinical validation

Among the 84 patients of EUREKA I who underwent RP, had adjuvant hormone therapy for more than 6 months, no radiotherapy, no neo-adjuvant therapy, we selected the 5 patients with a recurrence during the adjuvant therapy. Only 2 of them started with initial PSA value under the threshold of 0.2 mg/mL.

We used these 2 patients for a preliminary validation of the LHRH model (Fig 4a and 4b). Moreover, as a control, we selected a patient with no recurrence during ADT (Fig 4c).

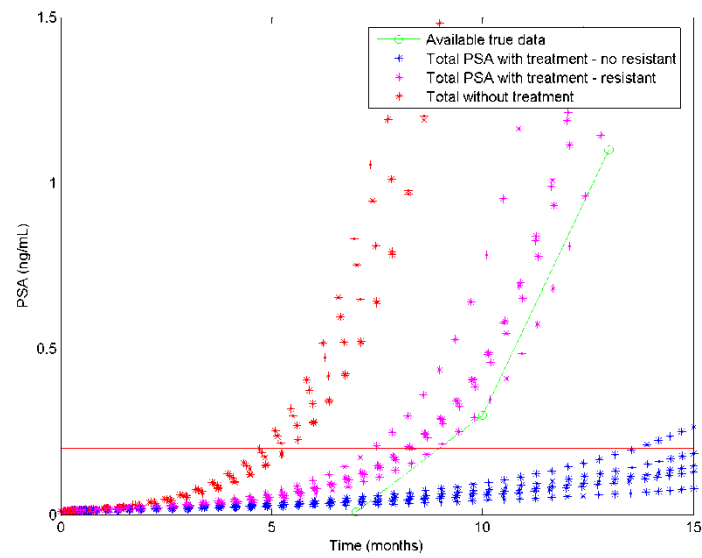


Fig4a Patient 1089 (no genetic information available)

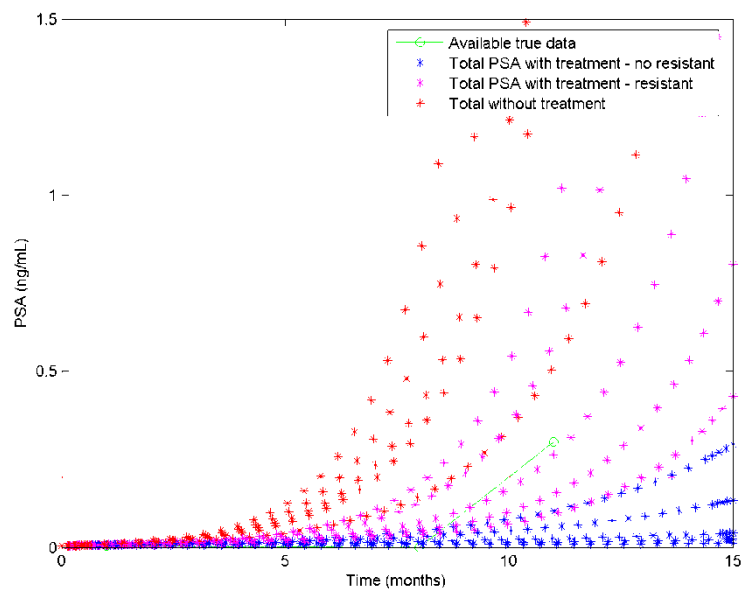


Fig4b Patient 2284 (no genetic information are available)

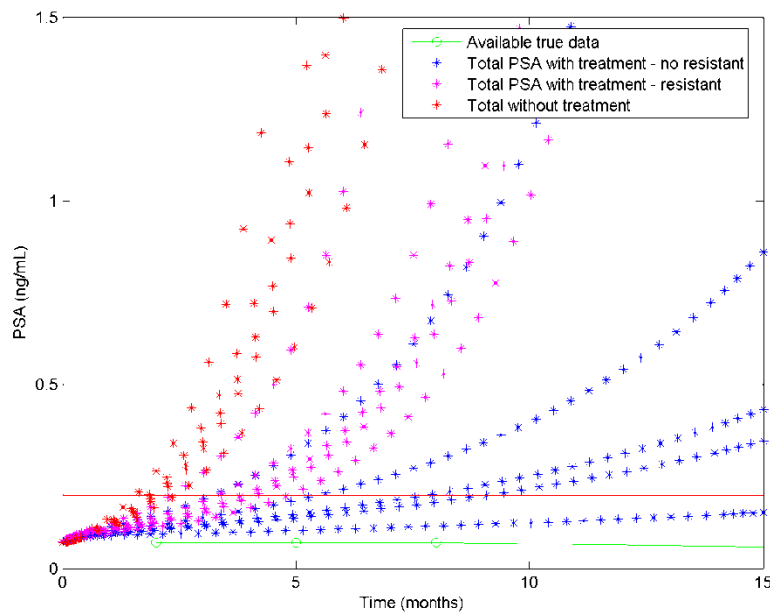


Fig4c Patient AA65 – under ADT

Our model shows 3 different scenarios: PSA without therapy (red stars), PSA during ADT in case of the presence of a resistant clone before the start of the therapy (magenta stars) and PSA during ADT in case of no resistant clone before the start of the therapy. Green dots are the real data of the patients.

As we expected, the two patients (Fig. 4a and 4b) with a recurrence during ADT are compatible with a huge resistant clone before starting therapy (magenta stars), while the patients who do not relapse (Fig. 4c) follows the blue stars. The testosterone level comes from ICCS models.

Our model gives 5 different previsions for each scenario, changing the parameter values according to their ranges. This happens because we want to give an idea of the behaviour of the PSA, but we cannot expect to predict the exact future PSA values. If extra information is available, for example gene expression, the prediction can be more accurate and the most probable scenario can be easy selected.

I.9 References

- M. Marberger et al., "Effectiveness, pharmacokinetics, and safety of a new sustained-release leuprolide a cetate 3.75-mg depot formulation for testosterone suppression in patients with prostate cancer: a Phase III, open-label, international multicenter study," *Clin. Ther.*, vol. 32, no. 4, pp. 744–757, Apr. 2010.
- J. Morken, A. Packer, R. Everett, J. Nagy, and Y. Kuang, "Mechanisms of resistance to intermittent androgen deprivation in patients with prostate cancer identified by a novel computational method," *Cancer Res.*, vol. 74, no. 14, pp. 3673–3683, 2014.
- H. Vierhapper, P. Nowotny, and W. Waldhäusl, "Determination of testosterone production rates in men and women using stable isotope/dilution and mass spectrometry," *J. Clin. Endocrinol. Metab.*, vol. 82, no. 5, pp. 1492–1496, 1997.

CHAPTER TE: TECHNICAL COMPONENTS AND THE WORKFLOW USED FOR THE VALIDATION OF THE CHIC INFRASTRUCTURE AS A WHOLE

(Please note that the numbering of sections, subsections, equations, figures and references within this chapter refers exclusively to the latter and is not applicable to other chapters of the document. If any of the above entities of another chapter is to be referred to, the chapter under consideration should also be mentioned through its two capital letter code such as “Chapter NB”)

I. The CHIC technical components and presentation of the workflow process

Even if the CRAF component is mainly used for the validation of the CHIC platform, all the CHIC technological components also play a significant role in the validation process, since they constitute the CHIC back end services on which the functionality of the CHIC platform depends. Thereafter, this chapter provides a brief description of all the CHIC components whose functionality is crucial for the storage of the hypomodels and the clinical data, the construction of the hypermodels, the execution of the simulation, the inspection of the results and finally the validation of the hypermodels and the CHIC platform as a whole. Since a detailed description of the following components has already been given in the corresponding past deliverables, this chapter mainly aims at providing a brief description of their functionalities and their contribution in the successful completion of all the CHIC workflows.

I.1 CRAF (Clinical Research Application Framework)

CRAF (Clinical Research Application Framework) is the main CHIC clinical front-end component. Its main objective is to integrate all the services offered by each and every CHIC component into a single application. The aforementioned application delivers to the clinician not only a collaborative interface for exchanging knowledge and sharing work, but also a comprehensive, valuable and user-friendly clinical tool which aims at serving as a clinical decision support (CDS) for the clinicians. Through CRAF, clinicians can take full advantage of all the underlying CHIC technology and basic science for the benefit of their cancer patients.

Since CRAF is the main entrance point to the CHIC platform with respect to the clinical domain, it needs to interact with almost all the other CHIC components. More specifically, CRAF interacts with the following CHIC components.

- **Model Repository:** CRAF makes use of the Model Repository’s web services in order to discover the different already developed hypermodels. The descriptive language in the form of xMML which defines the topology of the hypermodel, the description of the hypermodels, and the description of the hypermodel parameters can all be retrieved from the Model Repository and be presented to the clinician. It has to be noted that part of the aforementioned information is required by CRAF for preparing the execution of the models, while the rest of the information is needed in order to be presented to the clinicians (description of the hypermodels and their parameters, etc.).
- **In Silico Trial Repository:** The *In Silico* Trial Repository is the CHIC component which is used for persistently storing all the simulation scenarios and the *in silico* predictions. The special interfaces that have been developed for the *In Silico* Trial Repository enable the integration with CRAF. This integration offers the possibility to the clinician through CRAF

to both inspect the previous successfully finished *in silico* experiments and to store the new ones.

- Clinical Data Repository:** Since the Clinical Data Repository is the CHIC component which permanently hosts or the related medical data produced by the project, the interaction between the CRAF and the Clinical Data Repository is crucial. The aforementioned interaction which is achieved through the application programming interfaces of the repository facilitates the uploading procedure of new data sets in the clinical environment through CRAF. Apart from the uploading of new clinical data, CRAF interacts with the Clinical Data Repository so as to deliver to the clinician the list of the available patients whose clinical data can be exploited and processed by the desired hypermodel.
- VPH-HF:** Since the execution of the CHIC hypermodels is conducted by the VPH-HF framework, the cooperation between the CRAF and the VPH-HF is a *sine qua non*. After the selection of the desired hypermodel and the patient and upon pressing the CRAF button for the execution of the *in silico* experiment, the control is temporarily passed to the VPH-HF component for the execution of the simulation. This implies that the resource locators of all the patient data objects and the hypomodels that constitute the hypermodel, as well as the values of the input parameters of the hypermodel are all reached to the VPH-HF component through its software interfaces.
- CHIC Semantic Infrastructure:** Since the selection of the specific patient data to be used in each simulation and the checking on the values of the hypermodel parameters require intelligent decisions to be made, the connection between the CRAF and the semantics infrastructure is of utmost importance. The CHIC semantics infrastructure contains the semantic knowledge with respect to the clinical data and the hypermodels in a machine-readable way.
- CHIC Security Framework:** The CHIC security framework deals with all the security aspects of CHIC's technological platform, ranging from user authentication, authorization, and auditing, to data integrity and privacy, pseudoanonymization and reidentification of patient data. The widely accepted security standards facilitate the integration between the CRAF and the security framework in order to assure and enforce the legal and regulatory compliance within the CHIC clinical domain.

The architecture of the CHIC clinical domain and CRAF is depicted in the following figure:

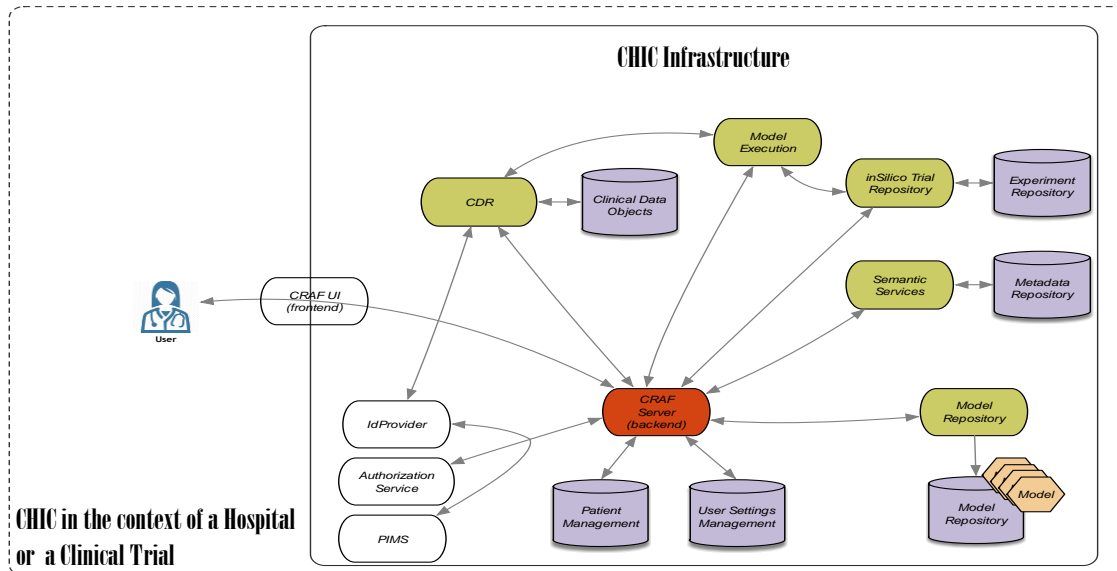


Figure A: The architecture of the CHIC clinical domain and CRAF as its core. The CRAF component is a web application which can be accessed through the browser although a desktop version of it is also available. Some screenshots that represent some of its services available to the end-users are depicted in the following figures. More specifically, figure B depicts the main CRAF window, figure C depicts the patient selection step, while figure D presents the step where the clinician selects the desired hypermodel.

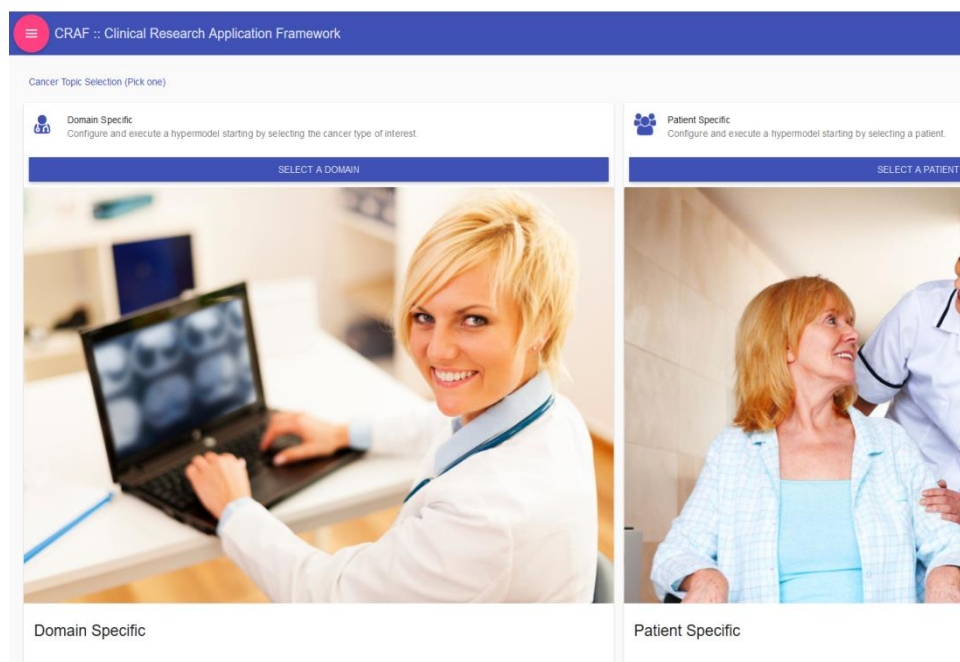


Figure B: The main page of the CRAF

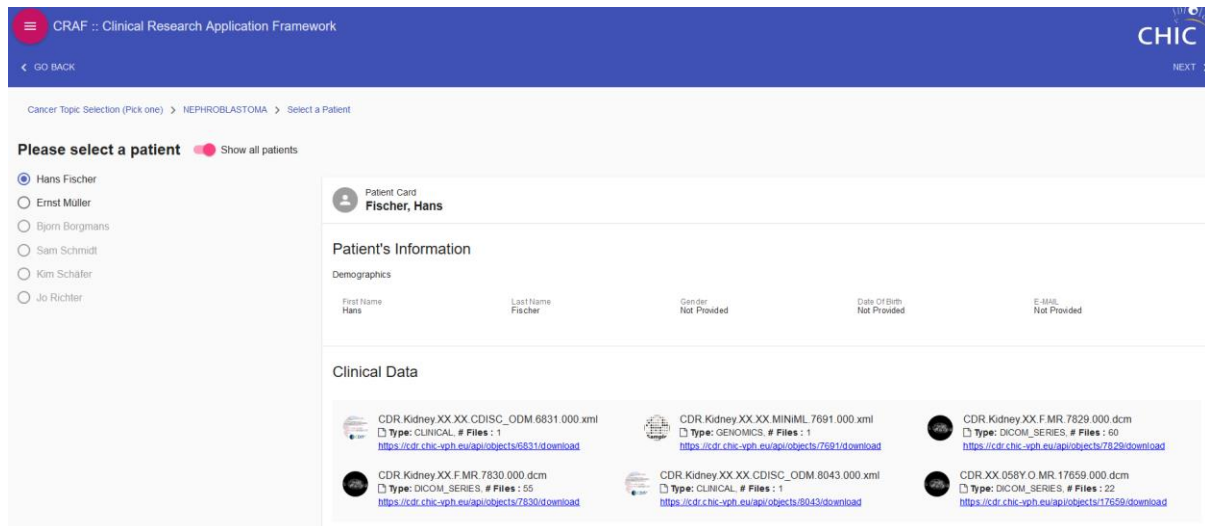


Figure C: Selection of a patient for nephroblastoma

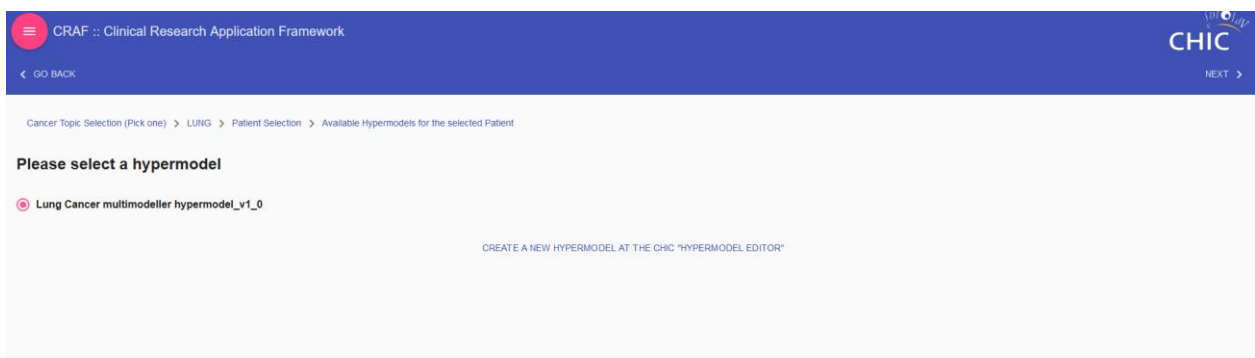


Figure D: Selection of the lung cancer multimodeller hypermodel

1.2 Model and Tool Repository

The CHIC Model and Tool Repository is the CHIC component that permanently hosts the models that have been developed in the context of the CHIC project. It is also able to host tools, linkers and data transformation tools necessary for the construction of the hypermodels. Such a tool is the preprocessing tool which is already stored in the Model Repository and performs the cropping, the interpolation and the 3D reconstruction of the initial metaimages. For each model/tool the Model Repository contains the following

- Description of the model
- Description of the model's input/output parameters

- Information related to the categorization of the model based on the CHIC I3 perspective approach
- Files of the model (executables, documentation, etc.)
- Information about model authorship, ownership and access permissions

In order for the user to interact with the repository, a web-based interface has been designed and implemented. Apart from the aforementioned graphical interface, many web services have been developed so as to be able to expose the contents of the repository to the other tools developed within the CHIC project, such as the Hypermodelling Editor, the CRAF, and the Hypermodelling Framework. The web services of the Model Repository have been extensively described in the deliverable 8.3 entitled “Implementation of the interfaces of the CHIC repositories”. Up to now, more than 15 hypomodels and 6 hypermodels exist in the Model Repository. All the aforementioned models can be accessed not only through the user interface of the repository, but also through the interface of the other CHIC components, such as the CRAF and the editor. As shown in the following figures, the user is able through the Model Repository to add a new model by using a 5-step wizard, inspect the models, update them, and filter them based on the I3 perspectives that have been described within the CHIC project.

The Model Repository has been fully integrated with the CRAF component through its developed HTTP based application programming interfaces. Thereafter, CRAF is able to retrieve from the Model Repository information related to the available hypermodels. The aforementioned information may be displayed to the clinicians through CRAF in order for them to select the desired hypermodel, run the simulation and get an answer for the clinical question.

ICCS: Lung Oncosimulator

Choose action for this model ▾

ID	UUID	Description	Comments	Version	String consisted of flag-value pairs	Name of the executable	Strongly coupled	Composite model	Freezed	Semantic information URL	Created on	Modified on
16	db6d173c-ad7c-11e5-8761-fa163e092aac	Simulation model of lung tumor growth and response to treatment(chemo + radio)		1	None	None		No	Yes	https://mr.chic-vph.eu/metadata#db6d173c-ad7c-11e5-8761-fa163e092aac	July 2, 2015, 4:34 p.m.	July 7, 2015, 2:10 a.m.

UOXF: Vasculature Model

Choose action for this model ▾

ID	UUID	Description	Comments	Version	String consisted of flag-value pairs	Name of the executable	Strongly coupled	Composite model	Freezed	Semantic information URL	Created on	Modified on
17	db6d1a6f-ad7c-11e5-8761-fa163e092aac	Model for transport and growth in the vasculature.		1	None	None		No	No	https://mr.chic-vph.eu/metadata#db6d1a6f-ad7c-11e5-8761-fa163e092aac	July 3, 2015, 5:01 p.m.	None

Figure E: The lung oncosimulator and the vasculature are displayed to the user through the graphical interface of the Model Repository

Parameters of the model: UNIBE: BiomechanicsSimulator												
Add one more parameter for this model												
Action	ID	UUID	Name	Description	Data type	Unit	Flag used to read static input parameter	Data range	Default value	Is mandatory	Is output	Is static
Action ▾	151	1b7a6f85-ad7d-11e5-8761-fa163e092aac	out_phi	Angles phi, theta relative to current cell in tumour growth domain where pressure is lowest.	number		None			No	Yes	No
Action ▾	152	1b7a7087-ad7d-11e5-8761-fa163e092aac	in_total	Concentration of biological cells in given computational cell of tumour growth domain.	number		None			Yes	No	No
Action ▾	248	1b7b4270-ad7d-11e5-8761-fa163e092aac	out_theta	Angle theta of direction of least pressure	number		None			No	Yes	No
Action ▾	249	1b7b4360-ad7d-11e5-8761-fa163e092aac	in_day	Simulation time point in days	number		None			No	No	No
Action ▾	363	eb251e48-aa74-11e5-91e4-fa163e092aac	path_to_simulation_domain	Vtk-readable segmentation file with organ labels. Labels for Nephroblastoma	file	valid file system path relative to	-s		/UNIBE_BMS/CHIC-SCENARIOS-LOCAL/NEPHROBLASTOMA/PATIENT_Demo/INPUT/CHIC_5XIHQQZ2GDYMIT55KON_TimePoint-1_labels_all_uchar.mhd	Yes	No	Yes

Figure F: The parameters of the biomechanics simulator are displayed to the user through the graphical interface of the Model Repository

Perspective I is about the Tumour-affected normal tissue modelling.
☐ I want to filter the available models based on Perspective I.

Perspective II is about the spatial scale(s) of the manifestation of life.
☐ I want to filter the available models based on Perspective II.

Perspective III is about the temporal scale(s) of the manifestation of life.
☐ I want to filter the available models based on Perspective III.

Perspective IV is about the closed form solution - algorithmic simulation modelling approach.
☐ I want to filter the available models based on Perspective IV.

Perspective V is about the tumour type(s) addressed.
☒ I want to filter the available models based on Perspective V.

Choose categories for Perspective V:

☐ lung cancer
☐ glioblastoma
☒ nephroblastoma
☐ colon cancer
☐ prostate cancer

Perspective VI is about the treatment modality(-ies) addressed.
☐ I want to filter the available models based on Perspective VI.

Figure G: The user filters the models that are related to nephroblastoma

I.3 *In Silico* Trial Repository

The *In Silico* Trial Repository is a crucial component of the CHIC platform since it can be used for validation purposes without the need to execute the same simulation again. This can be achieved by comparing the predictions based on the simulations that are stored in the *In Silico* Trial Repository with the actual quantitative therapy outcome of the patient that is stored in the clinical data repository. The aforementioned comparison for all the *in silico* experiments stored in the repository contributed in the evaluation and adaptation of all the hypermodels stored in the Model Repository. Thereafter, although the validation of the CHIC platform can be conducted through the CRAF component, the *In Silico* Trial Repository can also be used for evaluation and validation purposes. The main role of the repository is to persistently store the simulation scenarios and the *in silico* predictions. The input data (the original state of the patient), the simulation scenario (the hypermodel used in the simulation) and the output data (the state of the patient after the *in silico* treatment) are stored persistently after the execution of the hypermodel.

More specifically, the *In Silico* Trial Repository contains for each *in silico* trial the following information

- Model input of the simulation (preprocessed medical data)
- The hypermodel used in the simulation (not the actual hypermodel but a link to the corresponding record in the Model Repository)
- Model output (information related to the *in silico* prediction).

The content of the *In Silico* Trial Repository is available to the users (clinicians, modellers) either through the user interface that has been developed or through the corresponding web services. Consequently the user is able through the user interface of the repository or through the other CHIC components (CRAF, etc.) to easily store and retrieve all the data concerning a complete *in silico* trial (i.e. a set of simulation runs) that they or someone else has run. The two CHIC components that usually interact with the *In Silico* Trial Repository are the Hypermodelling Execution Framework, which stores the outcome of the simulation back to the repository, and the CRAF component which retrieves the results.

One of the main purposes of the *In Silico* Trial Repository is to test the repeatability and reproducibility of the experiments conducted in the context of *in silico* cancer domain. Repeatability is the ability for an individual to show that an experiment, repeated using the same material and equipment, yields the same result. In *in silico* medicine this means that if we run the same module multiple times on the same computer using the same software the same result would be yielded. Reproducibility is the ability for different individuals to show that an experiment repeated using different but similar material and different equipment yields the same statistical result. In *in silico* medicine this means that we are able to recreate a simulation without necessarily using the same software or computer that was used in the original simulation. Reproducing an experiment is one important approach that scientists use to gain confidence in their conclusions

The *In Silico* Trial Repository serves perfectly the aforementioned initiatives. By storing in one place the complete information concerning the input data, the output data, and the modules which participate in the *in silico* experiments and the *in silico* trials, the *In Silico* Trial Repository facilitates the evaluation and validation of the hypermodels stored in the Model and Tool Repository. [deliverable 8.1]

Special emphasis has been given during the development of the *In Silico* Trial Repository to provide a user interface where the user will need to provide minimal input for inspecting and evaluating the results of the *in silico* experiments. Figure H depicts the 5-step wizard used for storing a new *in silico*

experiment whereas figure I presents two of the *in silico* experiments that have been conducted with the nephroblastoma multimodeller hypermodel.

Wizard for storing a new experiment

Trial
Input Subject
Output Subject
Experiment
Experiment output files
Experiment input files
References related to the trial

References related to the experiment

All in silico experiments (simulations) that are part of the same in silico trial use the same in silico (hyper) model. This wizard step is about linking your simulation (experiment) with a trial and a (hyper) model.

Heads up! Please be aware that the selection of a model is obligatory. Furthermore, the description of the trial should not be empty before you submit the data of the new experiment.

Choose the name of the in silico model that is used in the trial: *
Choose name of the in silico model that is used in the trial
Type short textual description of the trial.
Short textual description of the trial *:
Type comments for this trial

Figure H: A screenshot of the wizard of the *In Silico* Trial Repository. This wizard is used for storing a new *in silico* experiment

This in silico experiment has been conducted with Nephroblastoma multimodeller hypermodel

Choose action for this experiment ▾

Experiment ID	Experiment UUID	Experiment Description	ID of the trial to which this experiment belongs	ID of input subject entity	ID of output subject entity	In the in silico experiment the "placebo model" must be used (yes/no)	Status of the in silico experiment	Comments	Experiment was created on	Experiment was modified on
666	7c56ff26-b0af-11e6-b95f-fa163e099cf4	Nephroblastoma multimodeller hypermodel	25	1310	1309		FINISHED SUCCESSFULLY	None	Nov. 22, 2016, 2:30 p.m.	Nov. 22, 2016, 2:53 p.m.

This in silico experiment has been conducted with Nephroblastoma multimodeller hypermodel

Choose action for this experiment ▾

Experiment ID	Experiment UUID	Experiment Description	ID of the trial to which this experiment belongs	ID of input subject entity	ID of output subject entity	In the in silico experiment the "placebo model" must be used (yes/no)	Status of the in silico experiment	Comments	Experiment was created on	Experiment was modified on
661	502ba118-690b-11e6-888d-fa163e099cf4	Nephroblastoma	25	1297	1298		FINISHED SUCCESSFULLY	None	Aug. 23, 2016, 11:26 a.m.	Aug. 23, 2016, 11:41 a.m.

Figure I: A screenshot of two in silico experiments that have been conducted with the Nephroblastoma multimodeller hypermodel

Moreover, the special interfaces (web services) that have been developed for the *In Silico* Trial Repository offer the possibility for the other CHIC components to retrieve the results of the stored simulations. Thereafter, based on the aforementioned repository interfaces, the clinician is able through CRAF to evaluate and validate the hypermodels.

1.5 Hypermodelling Framework

The building and deployment of a hypermodel is a complex process that requires the interaction of the user with many services developed in the CHIC hypermodelling infrastructure.

The first step is the creation of the hypomodels composing the hypermodel in the Model Repository. Each hypomodel has to be registered in the Model Repository together with the executables and library dependencies, the command-line arguments with the default values, the name of the executable and the kind of the model (for a reference on how to configure a hypomodel in the Model Repository see D8.4). Once all these information are provided by the User, the model is ready to be registered in the VPH-HF platform using the Registry service APIs (see Figure J).

In VPH-HF we distinguish two type of hypomodels based on the type of coupling (strongly coupled or not):

- Model of type A (strongly_coupled=**False**)
- Model of type B (strongly_coupled=**True**)

The registration process consists of two steps. In the first step of the registration process, the binaries and library dependencies are deployed in the computational infrastructure. In the second step, valid only for model of type A, the model metadata are fetched from the Model Repository and used for generating the model wrapper.

Once all the hypomodels are registered in the VPH-HF, the modeller can start building the hypermodel in the hypermodelling editor by linking graphically the available hypomodels. The graphical final result for the Nephroblastoma growth hypermodel is shown in Figure K. When the hypermodel composition is completed, an XML description of the hypermodel in the xMML format is generated and saved in the Model Repository together with the metadata.

If the hypermodel is composed only by hypomodels of type A, nothing more has to be done and it can be executed. If the hypermodel is composed only by hypomodels of type B, it has to be registered in the platform. The model metadata and the topology described in the xMML are used to generate the model wrapper and the Muscle configuration file (see Figure K). If a model is hybrid (an example of hybrid hypermodel is the Nephroblastoma growth hypermodel), which means it contains model of type A and B, only the strongly coupled part of the model needs to be registered.

Every kind of hypomodel or hypermodel is registered in the Jenkins Continuous Integration system for testing. If the test finishes without errors, the hypermodel is ready to be executed in VPH-HF by calling the Director APIs and providing the hypermodel description in xMML format and a valid input set. When the simulation is finished, the output results are uploaded and saved in the InSilicoTrial Repository for further analysis.

For any details on the Hypermodelling infrastructure, see D7.4.

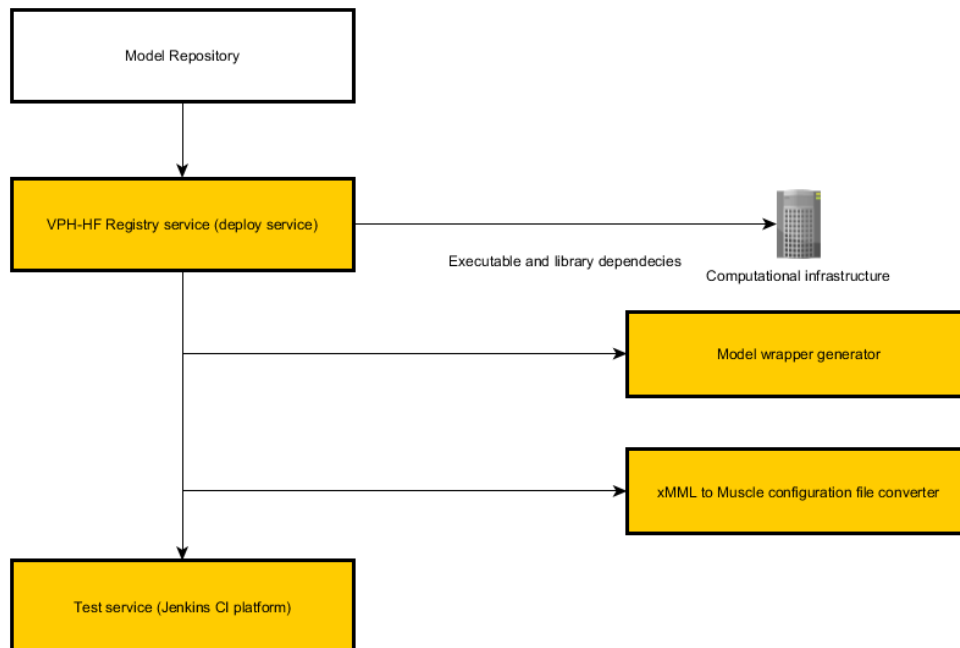


Figure J: Model registration services in VPH-HF

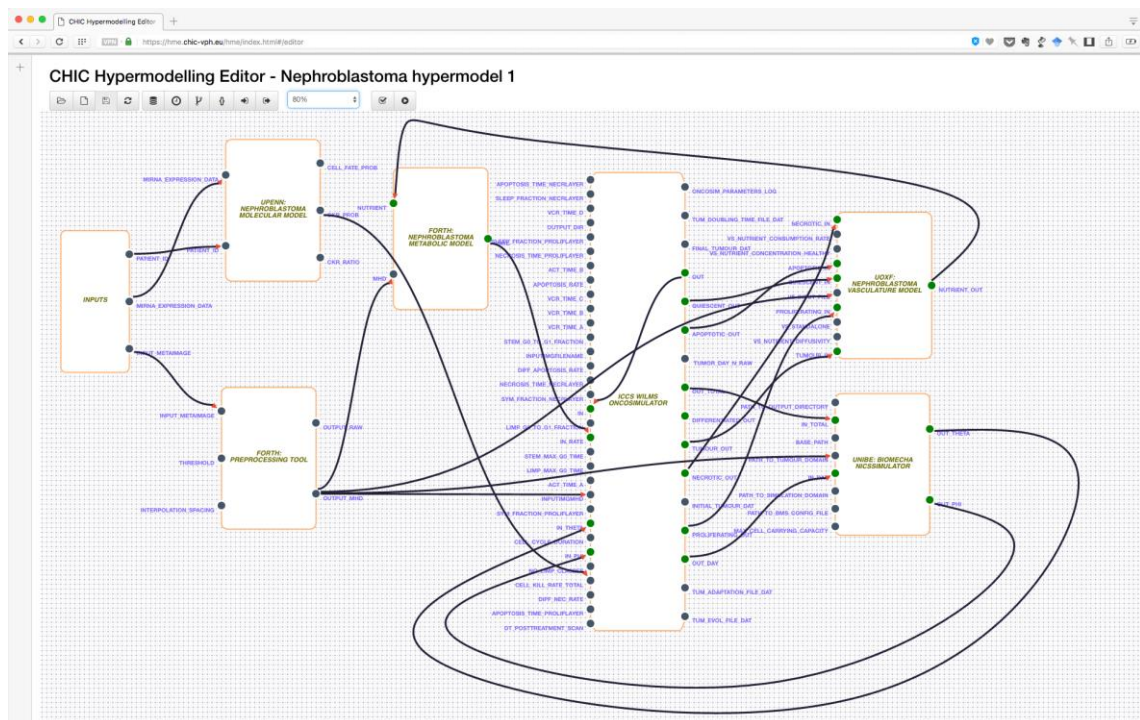


Figure K: The Nephroblastoma growth hypermodel representation in the Hypermodelling Editor

I.6 Clinical Data Repository

The CHIC clinical Data Repository is the CHIC component that permanently hosts all the related medical data that have been collected and produced during the CHIC project. The aforementioned data have passed de-identification and pseudo-anonymization processes. The CHIC Data Repository contains for each patient all the relevant medical data including clinical data, imaging data, histological data, therapy, etc. The data files that are hosted in the Data Repository are imaging data (DICOM, metaimages), clinical study data (CDISC-ODM), microarray gene expression data (MINiML) and other types of files (histological reports, etc.).

A web-based user interface has been developed for the Data Repository which serves as entry point for almost all functionalities described throughout the user guide introduced in the deliverable “D8.2: Prototype implementation of the CHIC repositories”. The following services are offered to the user through the graphical interface of the repository

- Storage and retrieval of pseudonymized clinical data
- Provision of data annotation such as ontology or object type/modality
- Linking of datasets to find related data
- Semantically driven search to find datasets containing the required anatomical structures
- Access control to the clinical data repository (single sign on, sharing of information, etc.)

Figure L presents the web-based user interface main view of the clinical data repository, whereas figure M outlines the dynamic search query builder integrated in the graphical interface. According to the aforementioned query builder, the user is able to conduct sophisticated search queries. More specifically, as shown in figure M, the user is able to find patients for whom we have imaging, clinical and miRNA nephroblastoma data.

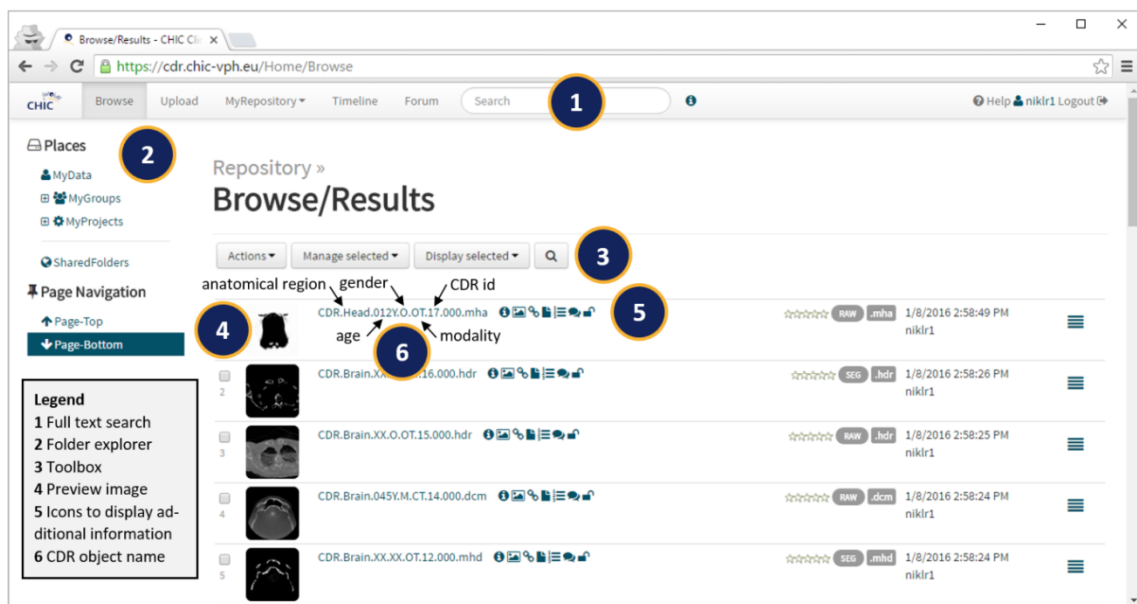


Figure L: The web-based user interface main view of the clinical data repository

Figure M: The dynamic search query builder integrated in the web-based user interface

During the upload process by the Clinical Data Repository, metadata can be extracted automatically, as long as standard file formats are used. The extracted metadata must be processed to triples before being exported to the Rdfstore. This is one of the reasons the clinical data repository stores the extracted metadata in the relational database. Another reason is the export process itself which requires a reliable retry logic. Last but not least, the clinical data repository needs to be able to display the information associated with each object without fetching it from the Rdfstore every time. The Rdfstore itself already offers the functionality to add and delete triples in order to enable interactions with the clinical data repository. Figure N presents the user dialog which is used by the Clinical Data Repository in order to annotate an object with anatomical regions using the autocomplete function offered by the Local Ontology Lookup Service (LOLS).

Figure N: User dialog to annotate an object with anatomical regions using the autocomplete function offered by the Local Ontology Lookup Service (LOLS)

Apart from the user interface of the Clinical Data Repository, special RESTful web services have been developed for the latter in order for the CHIC clients to be able to access the contents of the repository. The aforementioned web services facilitate the integration of the repository with CRAF and therefore, the clinician does not necessarily need to access different CHIC components in order to inspect the clinical data, to run the *in silico* experiments or to validate the CHIC platform. For a more concrete presentation of the CHIC Clinical Data Repository, reference can be made to the deliverables

I.7 Workflow used for the validation of the CHIC platform

The previous subchapters dealt with the presentation of the various CHIC technical components (repositories, execution framework, etc.). Even if the clinician conducts the validation through the CRAF component, all constituents of the CHIC platform are engaged in the validation workflow. Every CHIC component undertakes a certain role in the background or the foreground, and the successful completion of the CHIC workflows depends on the prosperous operation of every single part. For instance a malfunction in the Hypermodelling Framework may result in inability to run the hypermodel whereas a malfunction in the Clinical Data Repository may result in not being able to inspect the clinical data of a specific patient through CRAF. Moreover, a defect in the Model Repository may cause problems to CRAF with respect to the retrieval of the available hypermodels, whereas a flaw in the *In Silico* Trial Repository may increase the probabilities for not storing certain *in silico* predictions. Thereafter, this chapter presents the workflow needed for conducting the validation of the CHIC platform and the cooperation between the CHIC components. As shown in the following sequential diagram (figure O) the clinician is using CRAF through the browser. In order for CRAF to successfully operate it exchanges messages with almost all the CHIC components (Hypermodelling Execution Framework, Model Repository, Clinical Data Repository and *In Silico* Trial Repository). More specifically the workflow consists of the following steps:

- **Step one:** The clinician provides their credentials in CRAF in order to be logged in.
- **Step two:** The clinician selects a patient. (For this step a connection to the Clinical Data Repository needs to be established by CRAF).
- **Step three:** The clinician selects a hypermodel (For this step a connection to the Model Repository needs to be established by CRAF).
- **Step four:** The clinician selects the treatment plan.
- **Step five:** The clinician presses the button for starting the execution of the *in silico* experiment.
- **Step six:** The CRAF sends the corresponding messages to CRAF for the execution of the hypermodel.
- **Step seven:** The Hypermodelling Execution Framework retrieves the hypermodel description in the form of xMML from the Model Repository.

- **Step eight:** The Hypermodelling Execution Framework retrieves the description of the hypomodels (along with their executables) from the Model Repository (this step may be repeated many times).
- **Step nine:** The Hypermodelling Execution Framework retrieves from the Clinical Data Repository the clinical data of the selected patient.
- **Step ten:** The Hypermodelling Execution Framework executes the hypermodel.
- **Step eleven:** The hypermodelling Execution Framework stores the results of the *in silico* experiment in the *In Silico* Trial Repository.
- **Step twelve:** The hypermodelling Execution Framework notifies CRAF about the completion of the simulation.
- **Step thirteen:** CRAF retrieves the results of the *in silico* experiment from the *In Silico* Trial Repository.
- **Step fourteen:** The results are presented to the clinician. The clinician compares the prediction with the actual quantitative therapy outcome of the patient. Based on the aforementioned comparison and based on the performance of the CHIC platform, the CHIC platform is validated as a whole.

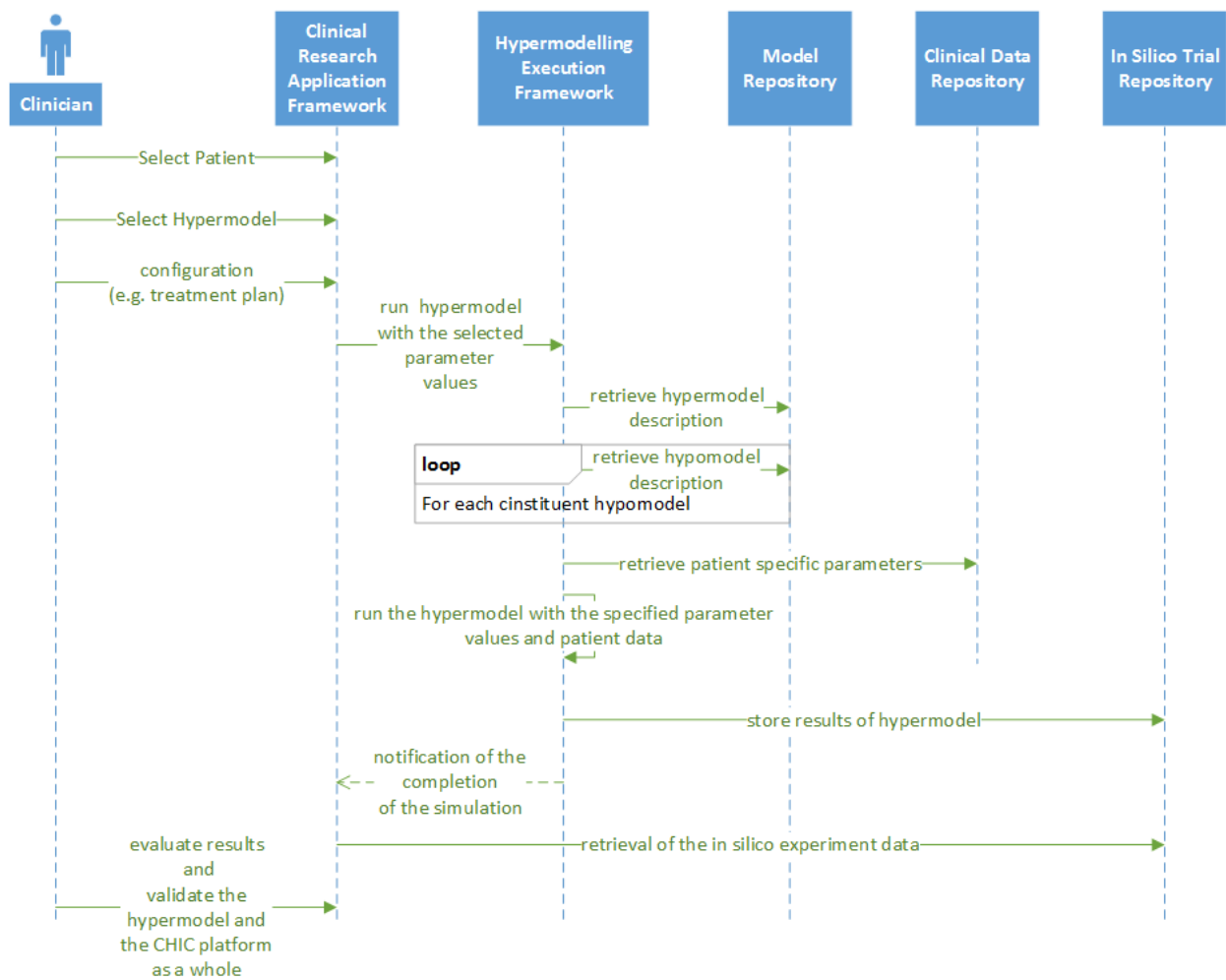


Figure O: Workflow used for the validation of the CHIC platform as a whole

CHAPTER DI: DISCUSSION

In this document the validation of the CHIC infrastructure as a whole has been reported. Validation has been achieved through the utilization and the execution of the three most computationally demanding clusters of highly innovative cancer *multimodeller*-hypermodels that have been developed by the CHIC project on the CHIC infrastructure. These multiscale hypermodels address nephroblastoma, non small cell lung cancer and prostate cancer. The paradigmatic cancer types considered are treated with a variety of modalities including chemotherapy, radiation therapy and hormone therapy. The adoption of several real clinical scenarios as the simulation execution context for the infrastructure validation procedure has rendered the latter clearly *clinically* relevant and *clinically* informative.

Various testing and validation actions, addressing *inter alia* execution outcome reproducibility, have been reported. This is a particularly important aspect, especially for those hypermodels which make use of (pseudo)random numbers through random number generators. In specific exemplary cases, it has also been shown how the utilization of the infrastructure can support the conduction of the scientific validation of a hypermodel.

In the last chapter of the document (TE) the technical components and the workflow used for the validation of the CHIC infrastructure as a whole have been outlined.

The overall outcome of the validation process under consideration has been a successful one. A stable functioning of the CHIC infrastructure has been achieved via an intensive and lengthy error identification and fixing procedure as is common in software engineering.

At this point it is recalled that the evaluation of the CHIC infrastructure and platform directly by the clinical community has already been reported in previous deliverables and therefore has not been part of the present document.

CHAPTER CO: CONCLUSIONS

In order to test and validate the CHIC infrastructure as a whole, extensive use of the highly innovative multimodeller hypermodels developed by CHIC in conjunction with a specially designed validation workflow have been made.

The overall outcome of the process of validation of the CHIC infrastructure as a whole has been a successful one. Proper functioning of the infrastructure has been achieved through an iterative series of intensive and lengthy error identification and fixing procedures. Technology developers, modellers and clinicians in close interaction and collaboration have all contributed to this successful outcome.

APPENDIX I: FREQUENT CHIC RELATED ABBREVIATIONS AND ACRONYMS

IMPORTANT NOTE: Abbreviations and acronyms that are not included in this table may be deciphered using the “Find” facility which is provided by current pdf document readers. By locating the first instance of an abbreviation or an acronym in the document, the reader can also see its full name

AD	Androgen Dependent
ADC	Adenocarcinoma
ADSCC	Adenosquamous Cell Carcinoma
ADT	Androgen Deprivation Therapy
AJCC	American Joint Committee on Cancer
Akt	Protein kinase B (PKB)
ALK	Anaplastic Lymphoma Kinase
AMD	Advanced Microdevices
ANSI	American National Standards Institute
API	Application Program Interface
ATP	Adenosine Triphosphate
AUC	Area Under Curve
BED	University of Bedfordshire
bGS	biopsy Gleason Score
BMS	Bio-Mechanical Simulator
BS	Biomechanics Simulator
CGAL	Computational Geometry Algorithms Library
CHIC	Computational Horizons in Cancer
CINECA	Consorzio Interuniversitario del Nord Est Italiano Per il Calcolo Automatico (Interuniversity Consortium for High Performance Systems)
CKP	Cell Kill Probability
CKR	Cell Kill Rate
CNS	Central Nervous System
COSMIC	Catalog of Somatic Mutations in Cancer
CRAF	Clinical Research Application Framework (CRAF)
CS	Cell Simulator
CSF	Cerebrospinal Fluid
CSS	Cancer Stem Cell
CSV	Comma Separated Values
CT	Computed Tomography
DC	Dendritic Cell
DGM	Diffusion Coefficient of Grey Matter
DICOM	Digital Imaging and Communications in Medicine
DIFF	Terminally Differentiated Cell
DRE	Digital Rectal Examination
DWM	Diffusion Coefficient of White Matter
EAU	European Association of Urology
EBRT	External Beam Radiation Therapy
ED	Equivalent Dose
EGF	Epidermal Growth Factor

EGFR	Epidermal Growth Factor Receptor
ERBB2	erb-b2 Receptor Tyrosine Kinase 2
ERK	Extracellular Signal-Regulated Kinases
FEM	Finite Element Method
FORTH	Foundation for Research and Technology Hellas
GBM	Glioblastoma Multiforme
GF	Growth Fraction
GC	Geometrical Cell
GPSM	Gleason, PSA, Seminal Vesicle and Margin Status
GS	Gleason Score
GUI	Graphical User Interface
HE	Hypermodelling Editor
HER3	Human Epidermal Growth Factor Receptor 3
HTML	Hypertext Markup Language
ICCS or ICCS- NTUA	Institute of Communication and Computer Systems – National Technical University of Athens
IMRT	Intensity Modulated Radiation Therapy
ISO	International Organization for Standardization
KUL	Catholic University of Leuven
LADC	Lung Adenocarcinoma
LCC	Large Cell Carcinoma
LIMP	Limited Mitotic Potential
LQ	Linear Quadratic
LSCC	Lung Squamous Cell Carcinoma
MAPK	Mitogen-Activated Protein Kinase
MD	Molecular Dynamics
MRI	Magnetic Resonance Imaging
MUSCLE	Multiscale Coupling Library and Environment
MUT	Mutant
NBC	Number of Biological Cells
NCCN	National Comprehensive Cancer Network
NCI	National Cancer Institute
NGCT	Neighbour Geometrical Cells belonging to the Tumour
NIH	National Institutes of Health
NK	Natural Killer
NSCLC	Non Small Cell Lung Cancer
NSG	NOD- <i>scid</i> <i>IL2r^{null}</i> Mouse Model of Human Skin
OER	Oxygen Enhancement Ratio
OFAT	One Factor at A Time
OS	Oncosimulator
OWL	Web Ontology Language
pAKT	phospho-AKT
PCa	Prostate Cancer
PDE	Partial Differential Equation
PSA	Prostate Specific Antigen
PUN	Phenomenological Universalities (Approach)
RDF	Resource Description Framework
RP	Radical Prostatectomy
RT	Radiotherapy
RTK	Receptor Tyrosine Kinase
SASA	Solvent Accessible Surface Area

SBML	Systems Biology Markup Language
SCC	Squamous Cell Carcinoma
SCID	Severe Combined ImmunoDeficient
SCLC	Small Cell Lung Cancer
SQL	Structured Query Language
STAT	Signal Transducer and Activator of Transcription or Signal Transduction And transcription
SVM	Support Vector Machines
TCGA	The Cancer Genome Atlas
TKI	Tyrosine Kinase Inhibitors
TRUS	Trans-Rectal Ultrasound
UBERN	University of Bern
UCL	University College London
ULC	Undifferentiated Large Cell Carcinoma
UML	Unified Modeling Language
UNITO	University of Turin
UOXF	University of Oxford
UPENN	University of Pennsylvania
USAAR	University of Saarland
USFD	University of Sheffield
VEGF	Vascular Endothelial Growth Factor
VPH	Virtual Physiological Human
VTk	Visualization ToolKit
WT	Wild Type
WT	Wilms Tumour = Nephroblastoma
XML	EXtensible Markup Language